

Serveur Académique Lausannois SERVAL serval.unil.ch

Author Manuscript

Faculty of Biology and Medicine Publication

This paper has been peer-reviewed but does not include the final publisher proof-corrections or journal pagination.

Published in final edited form as:

Title: Mfn2 downregulation in excitotoxicity causes mitochondrial dysfunction and delayed neuronal death.

Authors: Martorell-Riera A, Segarra-Mondejar M, Muñoz JP, Ginet V, Olloquequi J, Pérez-Clausell J, Palacín M, Reina M, Puyal J, Zorzano A, Soriano FX

Journal: The EMBO journal

Year: 2014 Oct 16

Volume: 33

Issue: 20

Pages: 2388-407

DOI: [10.15252/emboj.201488327](https://doi.org/10.15252/emboj.201488327)

In the absence of a copyright statement, users should assume that standard copyright protection applies, unless the article contains an explicit statement to the contrary. In case of doubt, contact the journal publisher to verify the copyright status of an article.

Mfn2 downregulation in excitotoxicity causes mitochondrial dysfunction and delayed neuronal death.

Alejandro Martorell-Riera¹, Vanessa Ginet⁴, Jesús Pérez-Clausell¹, Manuel Palacín^{2,3}, Manuel Reina¹, Julien Puyal⁴, Antonio Zorzano^{2,3}, Francesc X. Soriano^{1*}

1 Department of Cell Biology, 2 Department of Biochemistry and Molecular Biology, Faculty of Biology, University of Barcelona, Av. Diagonal, 643, 08028 Barcelona, Spain

3 Institute for Research in Biomedicine (IRB Barcelona), C/Baldiri Reixac 10, 08028 Barcelona, Spain

4 Département des Neurosciences Fondamentales, Université de Lausanne, Rue du Bugnon 9, 1005 Lausanne, Switzerland

* Correspondence to: Francesc X. Soriano, Department of Cell Biology, Faculty of Biology, University of Barcelona, Av. Diagonal, 643, 08028 Barcelona, Spain Tel. +34 934029046, Fax +34934034607. f.x.soriano@ub.edu

Abstract

Mitochondrial fusion and fission is a dynamic process critical for the maintenance of mitochondrial function and cell viability. During excitotoxicity neuronal mitochondria are fragmented but the mechanism underlying this process is poorly understood. Here we show that Mfn2 is the only member of the mitochondrial fusion/fission machinery whose expression is reduced in *in vitro* and *in vivo* models of excitotoxicity. Whereas in cortical primary cultures Drp1 recruitment to mitochondria plays a primordial role in mitochondrial fragmentation in an early phase that can be reversed once the insult has ceased, Mfn2 downregulation intervenes in a delayed mitochondrial fragmentation phase that progresses even when the insult has ceased. Downregulation of Mfn2 results in vulnerability of neurons to subtoxic doses of NMDA due to mitochondrial dysfunction and altered calcium homeostasis. We found that transcription factor MEF2 regulates basal Mfn2 expression in neurons, and that excitotoxicity-dependent degradation of MEF2 causes Mfn2 downregulation. Thus, Mfn2 reduction is a late event in excitotoxicity and its targeting may help to reduce excitotoxic damage and increase the currently short therapeutic window in stroke.

Introduction

Glutamate is the main excitatory neurotransmitter in the central nervous system. It plays an essential role in development, synaptic plasticity and neuronal survival but sustained elevated levels of extracellular glutamate kill neurons in a process called excitotoxicity (Arundine & Tymianski, 2003). Excitotoxicity takes place in both chronic neurological diseases, such as Huntington's and Alzheimer's disease, and in acute episodes such as traumatic brain injury and ischemic stroke. The NMDA receptor (NMDAR) is the main ionotropic glutamate receptor in the CNS and the excessive flux of Ca^{2+} that passes through it is a major cause of excitotoxicity. Despite evidence indicating a crucial role of NMDAR activation in brain damage during stroke, clinical trials with NMDAR blockers have failed because of poor tolerance and efficacy (Ikonomidou & Turski, 2002; Muir, 2006). In contrast to excessive NMDAR activity that causes cell death, its physiological activity triggers pro-survival signals that may play a role in promoting recovery and preventing delayed neuronal loss in the penumbra (Ikonomidou & Turski, 2002; Lo, 2008). Thus, future therapies to reduce excitotoxicity must target pro-death events downstream of NMDAR without affecting the pro-survival signals. Several mechanisms are implicated in cell death triggered by Ca^{2+} influx through NMDAR. Mitochondrial dysfunction caused by excessive Ca^{2+} uptake acts as a signaling hub for many pro-death events (Almeida et al, 1999; Reynolds & Hastings, 1995; Soriano et al, 2008; Stout et al, 1998; Yu et al, 2002).

Mitochondria are dynamic organelles that constantly fuse and divide, changing shape and localization. The equilibrium between fission and fusion is important for mitochondrial function, which is not only limited to supplying energy to the cell, but also intervenes in anabolic and catabolic biochemical pathways and the regulation of

Ca²⁺ homeostasis, and is a key regulator of cell death progression. The core mitochondrial fusion and fission machineries are formed by a group of dynamin-related large GTPases (Liesa et al, 2009; Westermann, 2010).

Inner mitochondrial membrane fusion is mediated by Opa1. Two Mitofusins (Mfn), Mfn1 and 2, mediate mitochondrial outer membrane fusion. Mfn1 and Mfn2 display high homology (81%) and around 60% identity, but nonetheless they have non-redundant roles (de Brito & Scorrano, 2008b; Liesa et al, 2009). In addition to its fusion role Mfn2 localization in the ER is necessary to maintain the reticular morphology of the ER and control the ER–mitochondria interaction (de Brito & Scorrano, 2008a). Mfn2 may also play a role in neuronal mitochondrial trafficking, and disruption of this function can lead to axon degeneration (Baloh et al, 2007; Misko et al, 2012). Mitochondrial fission is mediated by Drp1. Drp1 is mainly cytoplasmic and its translocation to mitochondria, recruited by Fis1 and/or Mff, is essential for mitochondrial fission. Drp1 is subjected to several posttranscriptional modifications, including phosphorylation, ubiquitination, SUMOylation and nitrosylation, which can either activate or repress fission activity (Cho et al, 2010; Oettinghaus et al, 2012).

Although mitochondrial fission per se does not cause cell death, fragmentation of mitochondria has been shown to play a key role in cell death progression. Mitochondrial fragmentation occurs early in apoptosis and can be delayed by expressing a dominant negative Drp1 (Breckenridge et al, 2003; Frank et al, 2001). Recently, Drp1 has also been implicated in the induction of necrosis (Wang et al, 2012). Mutations in Mfn2 are the most commonly identified cause of Charcot-Marie-Tooth type 2 (CMT2), a dominantly inherited disease characterized by degeneration of peripheral sensory and motor axons (Zuchner et al, 2004). Purkinje cells require Mfn2 but not Mfn1 for dendritic outgrowth, spine formation, and cell survival (Chen et al, 2007).

Mitochondrial fragmentation is an early event that occurs before the release of mitochondrial proteins and neurite degeneration in an *in-vivo* animal model of stroke (Barsoum et al, 2006). Despite the importance of mitochondrial dynamics in cell death progression the exact mechanism that underlies the mitochondrial fragmentation in excitotoxicity is incompletely understood. In this study, we assessed how the proteins of the core mitochondrial fission/fusion machinery are regulated in excitotoxicity. We found that Mfn2 levels are reduced in both *in-vitro* and *in-vivo* models of excitotoxicity, via MEF2 degradation that, by acting on the Mfn2 promoter, regulates basal levels of Mfn2. Downregulation of Mfn2 causes mitochondrial dysfunction and altered Ca^{2+} homeostasis, which sensitizes neurons to cell death.

Results

Mfn2 protein expression is reduced in excitotoxicity

Mitochondrial dynamics plays a pivotal role in cell death. Changes in mitochondrial morphology have been observed in excitotoxicity but the precise mechanism has not been fully defined. For a better understanding of the mechanism by which mitochondria are fragmented during excitotoxicity we exposed primary cortical cultures to moderate doses (30 μ M) of the glutamate receptor agonist NMDA over a time course of 1, 2, 4 and 8 hours and analyzed the expression of the proteins of the mitochondrial fission/fusion machinery. During the first 2 hours after NMDA application there were no significant changes in either fusion or fission proteins but after 4 hours of NMDA treatment we observed a 40% reduction in the fusion protein Mfn2 with no changes in the other fusion proteins, Mfn1 and Opa1. Surprisingly, Drp1 showed a tendency to reduce its protein levels during the first hour and reached a plateau thereafter (Fig. 1A,B). To rule out the possibility that changes in the expression of mitochondrial fission/fusion protein were due to changes in mitochondrial mass, volume normalization was also performed with the mitochondrial protein porin, achieving similar results (Fig. S1A).

To check the pathophysiological relevance of these *in vitro* findings we created an ischemic insult in P12 rats by permanent middle cerebral artery occlusion followed by 90 minutes occlusion of the carotid artery. During an ischemic episode, glutamate levels build up as a result of synaptic release and impaired and/or reversed uptake mechanisms (Camacho & Massieu, 2006), which induce excessive activation of NMDA glutamate receptors (NMDARs) and Ca^{2+} -mediated cell death (Arundine & Tymianski,

2003). We analyzed the expression of the mitochondrial fusion/fission machinery at several time points after the ischemic insult. The results were similar to those found *in vitro*. Two hours after restoration of the carotid blood flow, i.e. 3.5 hours after ischemia began, Mfn2 protein levels began to decline, and reached a significant 50% reduction 6 hours after the restoration of carotid blood flow (Fig. 1C,D and Fig. 1SB). Drp1 also showed a slight but significant reduction (20%) 2 hours after the restoration of blood flow. Neither of the other mitochondrial fusion proteins (Mfn1 and Opa1) showed changes in levels during the 24 hours after the onset of ischemia. Thus, our *in vitro* neuronal cultures recapitulate well the excitotoxic *in vivo* model.

Activation of Drp1 induces mitochondrial fragmentation

We observed Mfn2 downregulation 4 hours after initiating the insult, but nonetheless the kinetics of excitotoxicity-mediated mitochondrial fragmentation has been reported to be fast (Barsoum et al, 2006; Rintoul et al, 2003; Young et al, 2010). To clarify this, we analyzed the mitochondrial morphology of those neurons expressing RFP targeted to the mitochondrial matrix (mtRFP) that were still alive (as shown by nuclear DAPI staining; Fig. 2A) after NMDA treatment of different durations. Untreated neurons contained mainly well-connected tubular mitochondria (60%). After only 30–60 minutes of NMDA application most of the neurons contained globular mitochondria that remained intact for the following 2 hours, with a small amount of additional fragmentation 4 hours after NMDA treatment (Fig. 2B). Thus, although the secondary fragmentation correlates with the diminished Mfn2 expression it is unlikely that Mfn2 is responsible for the first, early phase of mitochondrial fragmentation.

We observed a tendency for a decline in Drp1 in excitotoxicity (Fig. 1). Nonetheless, what determines Drp1 activity is its subcellular localization. Drp1 is mainly cytosolic and by posttranslational modifications it is recruited to the mitochondria by Mff and/or Fis1 where it promotes fission (Gandre-Babbe & van der Blik, 2008; James et al, 2003; Otera et al, 2010; Yoon et al, 2003). In basal conditions GFP-Drp1 transfected neurons showed a weak diffuse signal within the neuron. Application of NMDA for 1 hour produced a strong punctuate signal that co-localized with mitochondria (Fig. 2C). Overexpression of a mutant form of Drp1 (Drp1-K38A), which acts as a dominant negative (Smirnova et al, 1998), or the Drp1 inhibitor mdivi-1, significantly attenuated the NMDA-mediated mitochondrial fragmentation during the first hour of NMDA treatment (Fig. 2D). Excitotoxic NMDA stimulates neuronal nitric oxide production, which nitrosylates and activates Drp1 (Barsoum et al, 2006; Cho et al, 2009). Consequently, inhibition of the nitric oxide synthase with 7-Nitroindazole (7-Ni) blocked the mitochondrial fragmentation to the same extent as the mutant Drp1-K38A or mdivi-1 (Fig. 2D). These experiments indicate that NO-mediated Drp1 activation plays a key role in mitochondrial fragmentation during excitotoxicity, although other mechanisms may also be involved.

Mfn2 intervenes in an irreversible late phase of mitochondrial fragmentation

Previous studies have shown that glutamate- and nitric-oxide-mediated mitochondrial fragmentation are amenable to restoration once the stimulus has ceased (Barsoum et al, 2006; Rintoul et al, 2003). Thereby, we decided to test the reversibility of mitochondrial morphology in our system. We applied NMDA for 1 hour and then washed out the NMDA and returned to fresh media. We observed that the mitochondrial tubular

morphology recovered 90 minutes after replacing the media but that after 180 minutes the mitochondria fragmented once again (Fig. 3A). The events that triggered the decline in Mfn2 levels began during the first hour of NMDA exposure since subsequent washout of the agonist did not block the reduction in Mfn2 (Fig. 3B). Because the delayed phase of mitochondrial fragmentation correlates with the reduction in Mfn2 protein levels (Fig. 1A, Fig. 2B and Fig. 3A, B) we reasoned that the reduction in Mfn2 levels in excitotoxicity intervenes in late mitochondrial fission. We knocked down Mfn2 using shRNA, which targets its sequence (shMfn2). Importantly, shMfn2 reduced Mfn2 protein levels by around 50%, resembling the reduction observed in excitotoxicity (Fig. 3C). As expected, knockdown of Mfn2 was sufficient to cause mitochondrial fragmentation (Fig. 3D and Fig. S2A, C). Another two shRNAs targeting Mfn2 at different sequences also showed mitochondrial fragmentation (Fig. S2B, C). Conversely, exogenous expression of Mfn2 significantly blocked the late phase of mitochondrial fragmentation after NMDA washout (Fig. 3E).

All of this indicates that excitotoxicity promotes mitochondrial fragmentation by at least two mechanisms, a fast mechanism relying on Drp1 activation that lasts while the insult is present, and a late mechanism dependent on the reduction in Mfn2 expression that takes place hours after the insult is generated and persists independently of the removal of the insult.

Mfn2 downregulation causes mitochondrial dysfunction and altered Ca^{2+} homeostasis and sensitizes neurons to excitotoxic damage

The therapeutic window in ischemic stroke is only 4.5 hours from the onset of symptoms (Zhang et al, 2012). Thus, it would be of great interest to find novel late

events for therapeutic targeting. The fact that we observed a decline in Mfn2 protein levels 4 hours after excitotoxicity started, and given that in addition to its mitochondrial fusion activity Mfn2 has unique properties that are not shared with Mfn1, such as activating mitochondrial oxidative metabolism or tethering of mitochondria with the ER regulating Ca^{2+} homeostasis (Bach et al, 2003; Baloh et al, 2007; de Brito & Scorrano, 2008a; Pich et al, 2005), led us to hypothesize that Mfn2 reduction could play an active role in the progression of excitotoxic damage. Thus, we determined how lower levels of Mfn2 could affect mitochondrial function. We first determined mitochondrial membrane potential as an indicator of mitochondrial function. In concordance with observations made in other cell types (Bach et al, 2003; Soriano et al, 2006), mitochondria in Mfn2 KD neurons had around 15% lower mitochondrial membrane potential than control transfected cells, indicating impaired mitochondrial function (Fig. 4A). The impairment of mitochondrial function was exacerbated when neurons were challenged with doses of NMDA at the threshold of toxicity. Application of 15 μM NMDA produced a moderate loss in mitochondrial membrane potential that was greatly enhanced in Mfn2 KD neurons (Fig. 4A).

Because mitochondria play a key role in buffering the increase in cytosolic Ca^{2+} produced during excitotoxicity, which depends on proper mitochondrial membrane potential (Nicholls, 2009), we reasoned that Ca^{2+} homeostasis may be impaired in Mfn2 KD neurons. Under basal conditions Mfn2 KD neurons have a slightly higher cytoplasmic Ca^{2+} concentration (Fig. 4B, C). The application of NMDA produced an increase in cytosolic Ca^{2+} that was much greater in Mfn2 KD cells (Fig. 4B, C). Calpain is a Ca^{2+} dependent Ser protease that has been implicated in excitotoxic cell death. We analyzed spectrin cleavage after NMDA as a measure of calpain activity and found that

Mfn2 KD neurons showed increased calpain activation consistent with the increased cytoplasmic Ca^{2+} concentration (Fig. S3A).

Given that reduced levels of Mfn2 had a great impact on mitochondrial membrane potential and Ca^{2+} handling when neurons were treated with low doses of NMDA, we wondered whether the reduction in Mfn2 could have consequences for cell viability. This was indeed the case, as knockdown of Mfn2 sensitized neurons to subtoxic doses of NMDA (Fig. 4D). Another two shRNAs targeting Mfn2 at different sequences also showed sensitization to subtoxic doses of NMDA, ruling out the possibility of an off-target effect (Fig. S3B). In contrast, although overexpression of Mfn2 slightly increased neuronal cell death, indicating the importance of fine regulation, it reduced NMDA-induced neuronal death by almost two fold (Fig. S3C, D).

Together, these data support the notion that a reduction in Mfn2 causes mitochondrial malfunction, which increases the vulnerability of neurons to excitotoxic cell death.

Mfn2 is regulated at the transcriptional level in excitotoxicity

Next we investigated the mechanism by which Mfn2 expression is reduced in excitotoxicity. It is well known that Mfn2 is degraded by the proteasome in a Parkin dependent manner (Chan et al, 2011; Tanaka et al, 2010). We wondered whether the decrease in Mfn2 levels in excitotoxicity was due to its proteasomal degradation. Surprisingly, we found that pretreatment of neurons with the proteasome inhibitor MG-132 did not abolish the NMDA dependent reduction in Mfn2 (Fig. 5A, B) even when the concentration of MG-132 used (10 μM) promoted the accumulation of ubiquitinated proteins and effectively blocked the CCCP mediated degradation of Mfn2 (Fig. S4A

and B). Therefore we can conclude that excitotoxic dependent downregulation of Mfn2 is not dependent on proteasomal degradation.

Excitotoxicity causes changes in transcriptional programs (Cook et al, 2012; Zhang et al, 2007), which could be consistent with the slow effect of NMDA on Mfn2 expression. We investigated whether Mfn2 reduction was due to changes in its gene expression. Mfn2 gene expression showed an initial increase during the first hour after NMDA application, probably a defensive response to malfunctioning mitochondria. Mfn2 gene expression started to decrease during the second hour, reaching a plateau after 4 hours that remained steady for up to 8 hours of treatment and correlated with the time course of protein expression (Fig. 5C). The repression of Mfn2 expression is specific since Mfn1 and SESN2 expression were not affected by NMDA treatment (Fig. 5C). These data indicate that Mfn2 gene expression is downregulated during excitotoxicity, but do not rule out the possibility that other proteases could participate in the excitotoxicity mediated reduction in Mfn2. To verify that a transcriptional change is the main mechanism by which Mfn2 expression is reduced in excitotoxicity, we used the transcriptional inhibitor actinomycin D or the translational inhibitor cycloheximide. As expected, the use of these inhibitors reduced Mfn2 protein levels but additional application of NMDA did not produce a further reduction in Mfn2, as would be expected if a proteolytic process was responsible for NMDA-mediated Mfn2 downregulation (Fig. 5 D, E). Thus, all these sets of experiments clearly indicate that the main mechanism by which NMDA mediates Mfn2 downregulation is at the transcriptional level rather than being a proteolytic process.

Excitotoxicity mediated Mfn2 downregulation depends on MEF2

MEF2(A–D) are transcription factors that play an important role in neuronal development and viability (Flavell et al, 2008; Mao et al, 1999). During excitotoxicity MEF2s are cleaved by caspases generating DNA binding domains without the transactivation domain, which acts as a dominant negative interfering form (Li et al, 2001; Okamoto et al, 2002). Time-course analysis of protein extracts of cortical neurons exposed to NMDA or brains from rats that have been subjected to ischemia showed a reduction in MEF2A in a pattern that correlated well with Mfn2 expression (Fig. 6 A, B). All this raises the possibility that NMDA-dependent cleavage of MEF2s may be responsible for Mfn2 downregulation in excitotoxicity. Neurons expressing the DNA binding domain of MEF2 without the transactivation domain showed reduced expression of Mfn2 protein and mRNA (Fig. 6C, F). Consistent with the reduced expression of Mfn2, MEF2-DN transduced neurons contained fragmented mitochondria whose morphology was restored by expressing exogenous Mfn2 (Fig. 6D). Mitochondria of MEF2-DN expressing neurons showed reduced mitochondrial membrane potential that could be raised by overexpression of Mfn2 (Fig. 6E). All these results demonstrate that Mfn2 expression is regulated by MEF2 but do not answer the question of whether MEF2 degradation is the main factor mediating Mfn2 downregulation in excitotoxicity. Thus, we analyzed Mfn2 mRNA in neurons transduced with AAV coding MEF2-DN and observed that Mfn2 downregulation with respect to its control (GFP transduced) neurons was not additively enhanced when NMDA was applied, suggesting that they act in a common pathway (Fig. 6F). Together, these data demonstrate a crucial role of MEF2 in the excitotoxicity-dependent downregulation of Mfn2.

MEF2 directly regulates basal Mfn2 expression in neurons

Next, we investigated whether MEF2 could directly regulate Mfn2 expression. In promoter reporter assays MEF2-DN repressed the activity of human Mfn2 promoter in neurons but did not repress the activity of SESN2 promoter, consistent with the unchanged expression of SESN2 in excitotoxicity (Fig. 7A). The effect of MEF2-DN on the Mfn2 promoter was neuron specific since it did not affect the promoter activity in 10T1/2 fibroblasts, a cell line with far less expression of MEF2 than neurons (Fig. 7A and Fig. S5A). These results are consistent with a prevalent role of MEF2 in the regulation of basal Mfn2 expression in neurons.

Next we determined the *cis*-elements involved in the effects of MEF2 on the transcriptional activity of the Mfn2 promoter. In agreement with the low expression of MEF2 in 10T1/2 cells, over-expression of MEF2A strongly activated the Mfn2 promoter (Fig. 7B). Deletion analysis of the Mfn2 promoter identified the MEF2A activated region as being between -1332 and -668 relative to the transcription start site (Fig. 7B). Further deletions revealed that the response region was located between -1030 and -862 (not shown). The MEF2 transcription factors bind DNA in A/T rich sequences (Black & Olson, 1998). The sequence -1030/-862 contains two putative MEF2 binding sites (Fig. S5B). In order to show the functional role of these putative MEF2 binding sites we disrupted the A/T rich sequence, introducing C and G by directed mutagenesis (Fig. S5B). Mutation of BOX 1 did not modify the MEF2A induced promoter activation but mutation of BOX 2 cancelled the effect of MEF2A (Fig. 7C). These results indicated that BOX 2 is the *cis*-element required for MEF2A mediated activation of the Mfn2 promoter.

Since MEF2A was able to *trans*-activated the Mfn2 promoter, EMSA experiments were performed in order to ascertain whether MEF2A was bound to BOX 2. A DNA fragment encompassing BOX 2 was radioactively labeled, and incubated with nuclear

extracts of HeLa cells overexpressing MEF2A. MEF2A bound BOX 2 containing probe, inducing the typical double band mobility shift (Santalucia et al, 2001), but did not bind the mutated probe (Fig. 7D). The retarded bands were competed with a 25- or 100-fold excess of unlabeled oligonucleotide probe or 100-fold excess of a probe of the Glut4 promoter that has previously been shown to bind MEF2 (Santalucia et al, 2001), whereas the cold mutated probe was unable to compete with the retarded bands. In addition, an antibody against MEF2 supershifted the complex (Fig. 7E). The binding of MEF2A to the Mfn2 promoter *in vivo* was confirmed by chromatin immunoprecipitation assays (ChIP). To this end, cells were transfected with MEF2A, extracts were immunoprecipitated with an anti-MEF2A antibody and a fragment of the promoter containing BOX 2 was amplified by PCR (-1004/-828). Immunoprecipitates specifically amplified the Mfn2 promoter, indicating the *in vivo* binding of MEF2A to the Mfn2 promoter (Fig. 7F).

Bioinformatic analysis of 2.5 kb of the rat Mfn2 promoter identified that there were four putative MEF2 binding sites in the region spanning -2313/-1983 (Fig. S5C). We designed primers to amplify within this region and performed ChIP with anti-MEF2A antibody in rat cortical neurons unstimulated or stimulated with NMDA for 4 hours. We found that under basal conditions MEF2 was bound to this region but after NMDA stimulation there was no enrichment of this region with the chromatin immunoprecipitate (Fig. 7G). These observations support the hypothesis that MEF2 regulates basal transcription of Mfn2 in neurons and as a consequence of MEF2 degradation Mfn2 transcription is downregulated in excitotoxicity (Fig. 8).

Discussion

Mitochondria are dynamic organelles that continuously fuse and divide. Changes in mitochondrial dynamics have profound effects on mitochondrial function and therefore mitochondrial viability. Here, we have studied mitochondrial dynamics in excitotoxicity. Our findings show that most of the mitochondrial fragmentation occurs within the first hour following the excitotoxic insult. This early phase depends partially on Drp1 mitochondrial translocation and lasts as long as the stimulus is present. Four hours after initiation of the insult, and regardless of its removal, delayed mitochondrial fragmentation that correlates with the reduction in Mfn2 protein levels due to its transcriptional downregulation occurs. Loss of Mfn2 impairs mitochondrial function and sensitizes neurons to excitotoxic damage.

Mechanisms of mitochondrial fragmentation in excitotoxicity

Drp1 is subjected to several posttranslational modifications that regulate its fission activity. Neuronal depolarization activates CaMKI, which phosphorylates Drp1 at Ser 600, promoting mitochondrial fragmentation that is reversible once neurons repolarize (Han et al, 2008). The reversibility of Drp1-mediated mitochondrial fragmentation has also been observed in pathological conditions. Mitochondrial fragmentation induced by NO donors is a rapid and reversible process (Barsoum et al, 2006). Ca^{2+} influx through the NMDA receptor produces NOS activation, which has been implicated in nitrosative stress and cell death (Sattler et al, 1999). Nitrosative stress causes S-nitrosylation of Drp1 at Cys644, which enhances mitochondrial fission (Cho et al, 2009). In agreement with previous reports (Barsoum et al, 2006), we show that NOS inhibition partially blocks NMDA-mediated mitochondrial fragmentation. The degree of inhibition of the mitochondrial fragmentation achieved by NOS inhibitors is similar to that achieved

using genetic and pharmacological inhibitors of Drp1. That suggests the involvement of a mechanism other than Drp1 in the early phase of mitochondrial fragmentation. Opa1 is cleaved in a mitochondrial membrane potential dependent manner, promoting mitochondrial fission (Griparic et al, 2007; Ishihara et al, 2006; Song et al, 2007), but we were unable to detect changes in the proportion of short and long forms of Opa1 in excitotoxicity, either *in vitro* or *in vivo*. Another possibility is that excitotoxicity could promote the modification of lipids, which has been shown to affect mitochondrial dynamics ((Choi et al, 2006)). The possibility that as yet unknown posttranscriptional modifications inhibit the fusion machinery in excitotoxic conditions cannot be ruled out either.

Our data also indicate that Mfn2 intervenes in the delayed phase of mitochondrial fragmentation. Cultured rat primary cortical neurons exposed to excitotoxic doses of NMDA and *in vivo* middle cerebral artery occlusion in rats show reduced expression of Mfn2 but no changes in Mfn1 or Opa1. During the preparation of the manuscript two independent studies confirmed the downregulation of Mfn2 in excitotoxicity. Primary rat cortical neurons exposed to 3 hours of oxygen and glucose deprivation (OGD), another model of excitotoxicity, also produced a reduction in Mfn2 protein with no changes in Opa1 and an increase in Mfn1 expression (Wappler et al, 2013). In an *in vivo* study, a reduction in Mfn2, and also of Opa1 expression, was observed in mice subjected to MCAO (Kumari et al, 2012).

Dependence of neurons on Mfn2

Mfn1 can compensate for some but not all of the functions of Mfn2. Analysis of Mfn2 and Mfn1 knockout mice indicates that they have both redundant and distinct functions

(Chen et al, 2003; Chen et al, 2007). Unlike Mfn1, a lack of or defects in Mfn2 have a great impact on neuronal viability. Mfn2 mutations have been found to cause the dominantly inherited neurological disease Charcot-Marie-Tooth type 2A (CMT2A) (Zuchner et al, 2004). Defects in mitochondrial mobility and fusion have been proposed as the mechanism by which Mfn2 mutations cause CMT2A but this has not been fully established (Baloh et al, 2007). Mfn2 is required for postnatal development of the cerebellum (Chen et al, 2007). Conditional dopaminergic Mfn2 knockout neurons show that Mfn2, but not Mfn1, is essential for striatal projections and proper nigrostriatal circuit function (Lee et al, 2012; Pham et al, 2012).

Our results show that neurons with Mfn2 knocked down to levels similar to those produced in excitotoxicity have impaired mitochondrial function. Independently of its fusion activity, Mfn2 repression in myotubes impairs mitochondrial oxidative metabolism and mitochondrial membrane potential by interacting with and regulating the expression of some subunits of OXPOS complexes I, II, III and V (Bach et al, 2003; Pich et al, 2005; Segales et al, 2013). Mitochondria play a crucial role in regulating Ca^{2+} homeostasis. Mitochondrial Ca^{2+} uptake is mediated by mitochondrial inner membrane mitochondrial calcium uniporter (MCU), which is driven by mitochondrial membrane potential. Mitochondrial Ca^{2+} uptake uses the proton-motive force, thus competing with mitochondrial ATP synthesis. In addition, membrane Ca^{2+} ATPase activation, which is used to remove elevated intracellular Ca^{2+} , causes an additional energetic demand on the neuron (Nicholls, 2009). A severe bioenergetic deficit may be in part responsible for the sensitization of Mfn2-knocked-down neurons to NMDA doses in the threshold of toxicity. There are other possible mechanisms by which Mfn2 reduction may contribute to neuronal vulnerability that are based on its unique properties. For example, Mfn2 deficiency is associated with endoplasmic reticulum stress (Sebastián et al, 2012).

Another possibility is based on the capacity of Mfn2 to arrest the cell cycle in vascular smooth muscle cells via its p21^{ras} motif (Chen et al, 2004). In neurodegenerative diseases, as well as stroke, there is a noxious attempt to re-enter the cell cycle that is associated with neuronal death (Herrup & Yang, 2007). Whether Mfn2 could block this attempt to re-enter the cell cycle in neurons remains to be determined.

Mfn2 is transcriptionally downregulated in excitotoxicity

During recent years several groups have established the role of the ubiquitin/proteasomal system in stress-mediated Mfn2 degradation. Mitochondrial depolarization promotes Mfn2 ubiquitinylation and proteasomal degradation in a Parkin-dependent manner (Chan et al, 2011; Tanaka et al, 2010). In stress conditions JNK phosphorylates Mfn2 at Ser 27 which recruits the E3 ubiquitinating ligase Huwe 1, leading to its ubiquitination and degradation (Leboucher et al, 2012). Although excitotoxicity causes both mitochondrial depolarization and JNK activation (Borsello et al, 2003; Nicholls, 2009; Soriano et al, 2008), the reduction in Mfn2 protein levels was not blocked by inhibiting the proteasome. We found that the main mechanism implicated in Mfn2 reduction acts at the transcriptional level and does not seem to depend on enhanced proteolysis since inhibiting transcription or translation does not further reduce Mfn2 levels. We have shown that transcription factor MEF2 regulates basal Mfn2 transcription in neurons and that excitotoxicity-mediated MEF2 degradation (Li et al, 2001; Okamoto et al, 2002) results in transcriptional downregulation of Mfn2 (Fig. 8). MEF2 transcription factors play a pivotal role in brain development, synapse development and neuronal survival. The genetic program regulated by MEF2 that controls synaptic remodeling has been characterized (Flavell et al, 2008) but although

many studies have pointed to the importance of MEF2 in supporting neuronal viability (Li et al, 2001; Mao et al, 1999; Okamoto et al, 2002), the precise target genes are poorly defined. Here we demonstrate that Mfn2 is a novel MEF2 target gene that can mediate its prosurvival function.

Mitochondrial dynamics in neurodegeneration

Mitochondrial dysfunction and excitotoxicity are common features of adult-onset neurodegenerative disorders such as Alzheimer's, Parkinson's and Huntington's disease, some of them occurring primarily in the absence of genetic linkage. Alterations in mitochondrial dynamics have been reported in all these diseases (Itoh et al, 2013). Mfn2 is dynamically regulated, thus its misregulation could intervene in the pathogenesis of neurodegenerative disorders. Further studies are required to clarify the role of Mfn2 in the progression of chronic late-onset neurodegenerative disorders.

During an ischemic episode, glutamate levels build up as a result of synaptic release and impaired and/or reversed uptake mechanisms, which induce excessive activation of NMDA glutamate receptors (NMDARs) and Ca²⁺ mediated cell death (Arundine & Tymianski, 2003). The evolution of ischemic injury is progressive, lasting for minutes, hours and even days. The ischemic core refers to the irreversibly damaged tissue. Surrounding the ischemic core there is a damaged but potentially salvageable area termed the ischemic penumbra (Lo, 2008). Hence, the ischemic penumbra is the most clinically relevant therapeutic target. Currently the only approved treatment for acute ischemic stroke is thrombolysis with tissue plasminogen activator (tPA) administered within 4.5 hours of symptom onset (Zhang et al, 2012). It is of great importance to find novel targets to extend the therapeutic window. In this study we show that Mfn2

downregulation is a late event of excitotoxicity (4 hours after the excitotoxic insult). Neurons with reduced Mfn2 have dysfunctional mitochondria and altered Ca^{2+} homeostasis. That makes neurons susceptible to excitotoxic damage and suggests that Mfn2 downregulation could determine the fate of neurons in the penumbra area. Thereby, Mfn2 is a potential therapeutic target against excitotoxicity in acute episodes and chronic neurodegenerative diseases.

Materials and methods

Cell culture, transfection and determination of cell death

Cortical neurons from E21 Sprague Dawley rats were cultured as described previously (Soriano et al, 2008). Experiments were performed after a culturing period of 10–11 days during which cortical neurons develop a rich network of processes, express functional NMDA-type and AMPA/kainate-type glutamate receptors, and form synaptic contacts. Prior to stimulations and transfections, neurons were transferred from growth medium to a medium containing 10% MEM (Invitrogen), 90% salt-glucose-glycine (SGG) medium (SGG: 114 mM NaCl, 0.219 % NaHCO₃, 5.292 mM KCl, 1 mM MgCl₂, 2 mM CaCl₂, 10 mM HEPES, 1 mM glycine, 30 mM glucose, 0.5 mM sodium pyruvate, 0.1% phenol red; osmolarity 325 mosm/l). Transfections were performed with Lipofectamine 2000 (Invitrogen). For cell death determination neurons transfected with GFP plus the indicated expression vectors were treated with NMDA for 6 hours and fixed. Nuclei were stained with DAPI and cell death was determined by counting the number of DAPI-stained pyknotic nuclei as a percentage of the total transfected neurons.

10T1/2 and HeLa cells were maintained in Dulbecco's modified Eagle's medium supplemented with 10% fetal bovine serum in subconfluent cultures. Transfections were performed with either Lipofectamine 2000 (Invitrogen) or Fugene (Roche).

Focal ischemia model

All animal procedures were in compliance with the directives of the Swiss Academy of Medical Science and were authorized by the veterinary office of the Canton of Vaud. Anesthesia was induced with 2.5% isoflurane in a chamber and maintained during the operation with a mask using 2.5% isoflurane. Middle cerebral artery occlusion was

performed in 12-day-old male Sprague-Dawley rats as previously described (Vaslin et al, 2009). Briefly, after the skin incision, a small piece of bone was removed from over the main (cortical) branch of the left middle cerebral artery, which was electrocoagulated just below its bifurcation into the parietal and frontal branches. The left common carotid artery was then occluded with a clip for 90 minutes. Rat pups were maintained at 37°C in the induction chamber (2.5% isoflurane) while the left common carotid artery was occluded. The arterial clip was then removed, and the restoration of carotid blood flow was verified under a dissecting microscope before the skin incision was closed using tissue adhesive (Histoacryl, B. Braun, Tuttlingen, Germany). Rat pups were transferred back to their mother until sacrifice.

Rat pups were decapitated and the brains were removed in PBS containing 1 mmol/L MgCl₂ on ice. The cortex were dissected and collected in protein hypotonic lysis buffer (20 mmol/L HEPES, pH 7.4, 10 mmol/L NaCl, 3 mmol/L MgCl₂, 2.5 mmol/L EGTA, 0.1 mmol/L dithiothreitol, 50 mmol/L NaF, 1 mmol/L Na₃VO₄, 1% Triton X-100, and a protease inhibitor cocktail (Roche)). Tissues were homogenized and sonicated, and protein concentration was determined using the Bradford assay.

Plasmids and virus generation

The following plasmids have been described previously: the -1982/+45 Mfn2-Luciferase vector and its 5' deletion constructs (Soriano et al, 2012), SESN2-Luc (Papadia et al, 2008), and mtRFP (Legros et al, 2002). HA-Mfn2 was subcloned into the pEF vector at the BamHI/XbaI sites. The MEF2A expression vector was a gift from Pilar Ruiz-Lozano (Stanford University, USA), GFP-Drp1 was a gift from AM van der Bliek (UCLA, USA), Drp1-K38A-myc was Addgene plasmid 26049, deposited by Dr.

Chan, and Mfn2-myc was Addgene plasmid 23213, deposited by Dr. Chan (Chen et al, 2003)).

The vectors used to construct and package recombinant adeno-associated viruses (rAAVs) were provided by Dr. Bading (U. Heidelberg, Germany (Zhang et al, 2007)). For construction of pAAV-MEF2-DN the first 252 bp of the mouse MEF2D cDNA (a gift from E. Olson; U. Texas South Western, USA) were amplified using the primers: forward 5'- *ATA GGA TCC* ATG GGG CGA AAG AAG ATA CAA ATC ACA CGC ATA ATG GAT G -3' and reverse 5'- *ATA AAG CTT TCA CAG ATC TTC TTC AGA AAT AAG TTT TTG TTA* GGA GGG CCT CGT TTG AAA ATA AAA TC -3'. The amplified product contains sequences that produce BamHI and HindIII restriction sites at the 5' and 3' respectively (italics) and also for inserting a myc tag into the C terminus (bold). GFP in the rAAV-GFP vector was removed by BamHI/HindIII digestion and the MEF2-DN PCR product was cloned into the rAAV vector to express the first 84 amino acids of the N terminus of MEF2, which contains the DNA binding domain but not the transactivation domain. rAAV for shRNA expression contains the U6 promoter for shRNA expression and a CMV/chicken beta-actin hybrid promoter driving hrGFP expression. rAAV-shRNA targeting Mfn2 were made by swapping the sh-sc sequence of rAAV-sh-sc (gift from H. Bading) for the following sequences of the rat Mfn2 into the BamHI and HindIII sites: shMfn2: 5'- AGA GGG CCT TCA AGC GCC AGT-3', shMfn2.2: 5'- GGG AAG AGC ACC GTG ATC AAT-3', shMfn2.3: 5'- TCC TCA AGG TTT ATA AGA ATG-3'. All newly generated constructs were confirmed by sequencing.

Neurons were infected with rAAV at DIV4. Infection efficiencies were determined at DIV 10-11 by analyzing GFP fluorescence or immunocytochemical analysis; they ranged from 80 to 90% of the viable neurons.

Site-directed mutagenesis

Site-directed mutagenesis was performed using the *QuikChange[®] Site-Directed Mutagenesis Kit* (Stratagene) according to the manufacturer's instructions. The mutated sequences are shown in Fig. S5B.

Luciferase assay

Firefly luciferase-based reporter gene was transfected along with a Renilla expression vector (pTK-RL; Promega), and also, where relevant, MEF2-DN expression vector. Forty hours after transfection luciferase assays were performed using the Dual Glo assay kit (Promega) with Firefly luciferase-based reporter gene activity normalized to the Renilla control (pTK-RL plasmid) in all cases.

RNA isolation, RT-PCR and qPCR

RNA was isolated using an RNA extraction kit (Life Technologies). For qPCR, cDNA was synthesized from RNA using the SuperScript[®] III First-Strand Synthesis SuperMix (Life Technologies) according to the manufacturer's instructions. qPCR was performed in a StepOne Real-Time PCR System (Applied Biosystem) using GoTaq QPCR Master Mix (Promega) according to the manufacturer's instructions. The primers used were: Mfn2 -F: 5'- ATG TCA AAG GGT ACC TGT CCA-3', -R: 5'- CAA TCC CAG ATG GCA GAA CTT-3'; SESN2 -F: 5'- GGA TTA TAC CTG GGA AGA CC -3, -R: 5'- CGC AGT GGA TGT AGT TCC -3'; Mfn1 -F: 5'-CAA ACT GCA GCC ACC AAG T-3', -R: 5'- GTT GGC ACA GTC GAG CAA-3'; 18S -F: 5'-GTG GAG CGA TTT GTC TGG TT-3', -R: 5'-CAA GCT TAT GAC CCG CAC TT-3'. Expression of the gene of interest was normalized to 18S, a commonly used control.

Western blotting and antibodies

Total cell lysates were boiled at 100°C for 5 min in 1.5x sample buffer (1.5 M Tris pH 6.8; Glycerol 15%; SDS 3%; β -mercaptoethanol 7.5%; bromophenol blue 0.0375%). Gel electrophoresis was performed using 10% polyacrylamide gels. The gels were blotted onto PVDF membranes, which were then blocked for 1 hour at room temperature with 5% (w/v) non-fat dried milk in TBS with 0.1% Tween 20. The membranes were then incubated at 4°C overnight with the primary antibodies diluted in blocking solution: anti-Mfn2 (1:2000; Abcam), Mfn1 (1:250, Santa Cruz), Opa1 (1:1000; BD Biosciences), Drp1 (1:1000, BD Biosciences), MEF2A (1:750, Santa Cruz), Jun (1:1000, BD Biosciences), Actin (1:10000, Sigma) and Porin (1:100000, Abcam). For visualization of Western blots, HRP-based secondary antibodies were used followed by chemiluminescent detection on Kodak X-Omat film. Western blots were analyzed by digitally scanning the blots, followed by densitometric analysis (ImageJ). All analyses involved normalizing to a loading control, Actin and Porin.

Imaging studies

Cells were visualized using a TCS SP2 Leica confocal laser scanning microscope (Leica Lasertechnik GmbH, Mannheim, Germany) adapted to an inverted Leitz DMIRBE microscope at 37°C in a controlled 5% CO₂ atmosphere (Life Imaging Services). Pictures were acquired using a 63X (1.32 NA) Leitz Plan-Apochromatic objective. Images were analyzed using ImageJ software (Rasband, W.S., 1997-2012).

To quantify mitochondrial membrane potential neurons were loaded with 20 nM tetramethylrhodamine methylester (TMRM; Sigma) in SGG medium without phenol red. Transfected cells were identified by co-transfecting GFP expression plasmid.

Single cells were monitored, TMRM was excited at 540 nm and emission was measured using a 570 nm filter. The mitochondrial membrane potential was compared to that observed in surrounding untransfected neurons and subsequently expressed as a percentage of that observed in untransfected cells before NMDA stimulation.

For mitochondrial morphology analysis neurons were transfected with mitochondrially targeted RFP. After treatment neurons were fixed, and nuclei were stained with DAPI. The number of live neurons with tubular or fragmented mitochondria was counted.

Drp1 localization was determined by transfecting cortical neurons with GFP-Drp1 and mtRFP. Forty-eight hours after transfection neurons were treated when appropriate with 30 μ M NMDA and fixed.

Measurement of cytoplasmic Ca²⁺

AAV-sh-sc- or AAV-sh-Mfn2-transduced neurons were loaded with 5 μ M of the ratiometric Ca²⁺ indicator Indo-1 for 30 minutes at 37°C in SGG medium without phenol red. After two washes with PBS neurons were incubated for 15 additional minutes in order to allow de-esterification of Indo-1. Neurons were excited at 350 nm and the ratio of the emitted fluorescence values at 405 (Indo-1 Ca²⁺ bound) and 485 nm (Indo-1 Ca²⁺ free) was used as an index of [Ca²⁺].

Chromatin immunoprecipitation (ChIP)

Two 60 mm dishes were used for each treatment (approx 4.5×10^6 cells). Medium was removed and treated cells were washed with pre-warmed medium and incubated for 10 minutes at room temperature with 1% para-formaldehyde in pre-warmed medium, to crosslink proteins to DNA. The reaction was stopped by adding glycine to a final concentration of 125 mM for 5 min. Cells were washed twice with ice-cold PBS and harvested on ice in swelling buffer (25% HEPES pH 7.9, 1.5 mM $MgCl_2$, 10 mM KCl, 0.1% NP40 plus protease inhibitor cocktail set III (Calbiochem)). Nuclei were isolated using a douncer and centrifuging at 1500 g for 5 minutes. Nuclei were resuspended in 200 μ l sonication buffer (50 mM HEPES pH 7.9, 140 mM NaCl, 1 mM EDTA, 1% Triton X100, 0.25% NaDeoxycholate, 0.1% SDS plus protease inhibitors). The nuclei were sonicated using a Diagenode Bioruptor (Liege, full power 30 s on, 30 s off, in an ice bath for 20 min) to produce fragments < 500 bp. Sonicated chromatin was precleared with protein-A agarose beads/salmon sperm DNA for 1 h at 4°C with agitation, beads were collected by centrifugation and supernatants were collected and subjected to immunoprecipitation. Eight micrograms of anti-MEF2 (Santa Cruz) or anti-Rabbit IgG (control, Sigma) was added for overnight incubation at 4°C with agitation. After chromatin immunoprecipitation, DNA was precipitated using Qiagen DNA purification columns. Input (1% of total immunoprecipitated) and immunoprecipitated DNA were subjected to qPCR analysis with primers amplifying the Mfn2 promoter (-2204/-2136 of the rat Mfn2 promoter) 5'-TGG AGA TGG AAT TCA AGT TGG-3' forward and 5'-TGGTCACAAAATGGCTCAGT-3' reverse. As negative controls we used primers for amplification of the actin gene 5'-AGC CAT GTA CGT AGC CAT CC-3' forward and 5'-CTC TCA GCT GTG GTG GTG AA-3' reverse.

For binding to the human Mfn2 promoter, input and immunoprecipitated DNA were subjected to PCR analysis using the primers 5'-GTG CAG TGG CAT GAT CTC GGC TCA-3' and 5'-GGC GAG GCG GGT GCA TCG GGA GTT-3', which flank the MEF2 site on the human Mfn2 promoter, and the primers 5'-CAA ATG CTG GAC CCA ACA CAA-3' and 5'-CCT CCA CAA TAT TCA TGC CTT CTT-3', which flank a region of human cyclophilin gene.

Electrophoretic mobility-shift assays

HeLa cells were transfected with expression vector for MEF2A and 48 hours later, nuclear extracts were prepared as described previously (Santalucia et al, 2001). Radiolabeled double strand oligonucleotide probe containing the human Mfn2 promoter sequence (containing the MEF2 binding site: 5'-ATT TTT GTA TTT TTA GTA CAG-3' (MEF2wt), the mutated MEF2 binding site (in bold), which differs from the wild type in the same three nucleotides used in the luciferase assay: 5'-ATT TTT **GGA TCC TTA** GTA CAG-3' (MEF2mut), and the MEF2 binding site in the Glut4 promoter: 5'-CGT GGG AGC TAA AAA TAG CCA-3' (MEF2Glut4) was incubated with 10 µg nuclear extract in a final volume of 20 µl and electrophoresis was performed as described previously (Santalucia et al, 2001). Dried gel was exposed to Kodak film. Competitor mutated oligonucleotide differed from wild-type EMSA sequence by the same base substitution used in the functional experiments. For supershift assays, MEF2 antibody was added to the corresponding binding reactions after incubation with the radiolabeled probe, and incubated for a further 10 minutes at room temperature before loading onto gels.

Statistical analysis

Statistical testing involved two-tailed student T-tests. For any multiple comparisons within data sets we used a one-way ANOVA followed by the Bonferroni post-hoc test.

All data are presented as mean \pm s.e.m. of at least three independent experiments.

Acknowledgments

This work was supported by the Fundació La Marató de TV3 (111210; FXS) and Spanish Ministerio de Ciencia e Innovación (SAF2011-30283; FXS). FXS is a researcher from the Programa Ramón y Cajal funded by the Ministerio de Ciencia e Innovación (RYC-2009-05407).

Conflict of interest

The authors declare that they have no conflict of interest.

References

- Almeida A, Bolanos JP, Medina JM (1999) Nitric oxide mediates glutamate-induced mitochondrial depolarization in rat cortical neurons. *Brain research* **816**: 580-586
- Arundine M, Tymianski M (2003) Molecular mechanisms of calcium-dependent neurodegeneration in excitotoxicity. *Cell Calcium* **34**: 325-337
- Bach D, Pich S, Soriano FX, Vega N, Baumgartner B, Oriola J, Daugaard JR, Lloberas J, Camps M, Zierath JR, Rabasa-Lhoret R, Wallberg-Henriksson H, Laville M, Palacín M, Vidal H, Rivera F, Brand M, Zorzano A (2003) Mitofusin-2 Determines Mitochondrial Network Architecture and Mitochondrial Metabolism. *Journal of Biological Chemistry* **278**: 17190-17197
- Baloh RH, Schmidt RE, Pestronk A, Milbrandt J (2007) Altered Axonal Mitochondrial Transport in the Pathogenesis of Charcot-Marie-Tooth Disease from Mitofusin 2 Mutations. *The Journal of Neuroscience* **27**: 422-430
- Barsoum MJ, Yuan H, Gerencser AA, Liot G, Kushnareva Y, Graber S, Kovacs I, Lee WD, Waggoner J, Cui J, White AD, Bossy B, Martinou J-C, Youle RJ, Lipton SA, Ellisman MH, Perkins GA, Bossy-Wetzel E (2006) Nitric oxide-induced mitochondrial fission is regulated by dynamin-related GTPases in neurons. *Embo J* **25**: 3900-3911
- Black BL, Olson EN (1998) Transcriptional control of muscle development by myocyte enhancer factor-2 (MEF2) proteins. *Annual Review of Cell and Developmental Biology* **14**: 167-196
- Borsello T, Clarke PG, Hirt L, Vercelli A, Repici M, Schorderet DF, Bogousslavsky J, Bonny C (2003) A peptide inhibitor of c-Jun N-terminal kinase protects against excitotoxicity and cerebral ischemia. *Nat Med* **9**: 1180-1186
- Breckenridge DG, Stojanovic M, Marcellus RC, Shore GC (2003) Caspase cleavage product of BAP31 induces mitochondrial fission through endoplasmic reticulum calcium signals, enhancing cytochrome c release to the cytosol. *The Journal of Cell Biology* **160**: 1115-1127
- Camacho A, Massieu L (2006) Role of Glutamate Transporters in the Clearance and Release of Glutamate during Ischemia and its Relation to Neuronal Death. *Archives of Medical Research* **37**: 11-18
- Cook DJ, Teves L, Tymianski M (2012) Treatment of stroke with a PSD-95 inhibitor in the gyrencephalic primate brain. *Nature* **483**: 213-217
- Chan NC, Salazar AM, Pham AH, Sweredoski MJ, Kolawa NJ, Graham RLJ, Hess S, Chan DC (2011) Broad activation of the ubiquitin–proteasome system by Parkin is critical for mitophagy. *Human Molecular Genetics* **20**: 1726-1737

Chen H, Detmer SA, Ewald AJ, Griffin EE, Fraser SE, Chan DC (2003) Mitofusins Mfn1 and Mfn2 coordinately regulate mitochondrial fusion and are essential for embryonic development. *J Cell Biol* **160**: 189-200

Chen H, McCaffery JM, Chan DC (2007) Mitochondrial Fusion Protects against Neurodegeneration in the Cerebellum. *Cell* **130**: 548-562

Chen K-H, Guo X, Ma D, Guo Y, Li Q, Yang D, Li P, Qiu X, Wen S, Xiao R-P, Tang J (2004) Dysregulation of HSG triggers vascular proliferative disorders. *Nat Cell Biol* **6**: 872-883

Cho D-H, Nakamura T, Fang J, Cieplak P, Godzik A, Gu Z, Lipton SA (2009) S-Nitrosylation of Drp1 Mediates β -Amyloid-Related Mitochondrial Fission and Neuronal Injury. *Science* **324**: 102-105

Cho D-H, Nakamura T, Lipton S (2010) Mitochondrial dynamics in cell death and neurodegeneration. *Cellular and Molecular Life Sciences* **67**: 3435-3447

Choi SY, Huang P, Jenkins GM, Chan DC, Schiller J, Frohman MA (2006) A common lipid links Mfn-mediated mitochondrial fusion and SNARE-regulated exocytosis. *Nat Cell Biol* **8**: 1255-1262

de Brito OM, Scorrano L (2008a) Mitofusin 2 tethers endoplasmic reticulum to mitochondria. *Nature* **456**: 605-610

de Brito OM, Scorrano L (2008b) Mitofusin 2: A Mitochondria-Shaping Protein with Signaling Roles Beyond Fusion. *Antioxidants & Redox Signaling* **10**: 621-634

Flavell SW, Kim TK, Gray JM, Harmin DA, Hemberg M, Hong EJ, Markenscoff-Papadimitriou E, Bear DM, Greenberg ME (2008) Genome-wide analysis of MEF2 transcriptional program reveals synaptic target genes and neuronal activity-dependent polyadenylation site selection. *Neuron* **60**: 1022-1038

Frank S, Gaume B, Bergmann-Leitner ES, Leitner WW, Robert EG, Catez F, Smith CL, Youle RJ (2001) The Role of Dynamin-Related Protein 1, a Mediator of Mitochondrial Fission, in Apoptosis. *Developmental Cell* **1**: 515-525

Gandre-Babbe S, van der Bliek AM (2008) The Novel Tail-anchored Membrane Protein Mff Controls Mitochondrial and Peroxisomal Fission in Mammalian Cells. *Molecular Biology of the Cell* **19**: 2402-2412

Griparic L, Kanazawa T, van der Bliek AM (2007) Regulation of the mitochondrial dynamin-like protein Opa1 by proteolytic cleavage. *The Journal of Cell Biology* **178**: 757-764

Han X-J, Lu Y-F, Li S-A, Kaitsuka T, Sato Y, Tomizawa K, Nairn AC, Takei K, Matsui H, Matsushita M (2008) CaM kinase I α -induced phosphorylation of Drp1 regulates mitochondrial morphology. *The Journal of Cell Biology* **182**: 573-585

Herrup K, Yang Y (2007) Cell cycle regulation in the postmitotic neuron: oxymoron or new biology? *Nat Rev Neurosci* **8**: 368-378

Ikonomidou C, Turski L (2002) Why did NMDA receptor antagonists fail clinical trials for stroke and traumatic brain injury? *The Lancet Neurology* **1**: 383-386

Ishihara N, Fujita Y, Oka T, Mihara K (2006) Regulation of mitochondrial morphology through proteolytic cleavage of OPA1. *EMBO J* **25**: 2966-2977

Itoh K, Nakamura K, Iijima M, Sesaki H (2013) Mitochondrial dynamics in neurodegeneration. *Trends Cell Biol* **23**: 64-71

James DI, Parone PA, Mattenberger Y, Martinou J-C (2003) hFis1, a Novel Component of the Mammalian Mitochondrial Fission Machinery. *Journal of Biological Chemistry* **278**: 36373-36379

Kumari S, Anderson L, Farmer S, Mehta SL, Li PA (2012) Hyperglycemia Alters Mitochondrial Fission and Fusion Proteins in Mice Subjected to Cerebral Ischemia and Reperfusion. *Translational stroke research* **3**: 296-304

Leboucher GP, Tsai YC, Yang M, Shaw KC, Zhou M, Veenstra TD, Glickman MH, Weissman AM (2012) Stress-induced phosphorylation and proteasomal degradation of mitofusin 2 facilitates mitochondrial fragmentation and apoptosis. *Mol Cell* **47**: 547-557

Lee S, Sterky FH, Mourier A, Terzioglu M, Cullheim S, Olson L, Larsson N-G (2012) Mitofusin 2 is necessary for striatal axonal projections of midbrain dopamine neurons. *Human Molecular Genetics* **21**: 4827-4835

Legros F, Lombès A, Frachon P, Rojo M (2002) Mitochondrial Fusion in Human Cells Is Efficient, Requires the Inner Membrane Potential, and Is Mediated by Mitofusins. *Molecular Biology of the Cell* **13**: 4343-4354

Li M, Linseman DA, Allen MP, Meintzer MK, Wang X, Laessig T, Wierman ME, Heidenreich KA (2001) Myocyte Enhancer Factor 2A and 2D Undergo Phosphorylation and Caspase-Mediated Degradation during Apoptosis of Rat Cerebellar Granule Neurons. *The Journal of Neuroscience* **21**: 6544-6552

Liesa M, Palacín M, Zorzano A (2009) Mitochondrial Dynamics in Mammalian Health and Disease. *Physiological Reviews* **89**: 799-845

Lo EH (2008) A new penumbra: transitioning from injury into repair after stroke. *Nat Med* **14**: 497-500

Mao Z, Bonni A, Xia F, Nadal-Vicens M, Greenberg ME (1999) Neuronal Activity-Dependent Cell Survival Mediated by Transcription Factor MEF2. *Science* **286**: 785-790

Misko AL, Sasaki Y, Tuck E, Milbrandt J, Baloh RH (2012) Mitofusin2 Mutations Disrupt Axonal Mitochondrial Positioning and Promote Axon Degeneration. *The Journal of Neuroscience* **32**: 4145-4155

Muir KW (2006) Glutamate-based therapeutic approaches: clinical trials with NMDA antagonists. *Current Opinion in Pharmacology* **6**: 53-60

Nicholls DG (2009) Mitochondrial calcium function and dysfunction in the central nervous system. *Biochimica et biophysica acta* **1787**: 1416-1424

Oettinghaus B, Licci M, Scorrano L, Frank S (2012) Less than perfect divorces: dysregulated mitochondrial fission and neurodegeneration. *Acta Neuropathol* **123**: 189-203

Okamoto S-i, Li Z, Ju C, Schölzke MN, Mathews E, Cui J, Salvesen GS, Bossy-Wetzel E, Lipton SA (2002) Dominant-interfering forms of MEF2 generated by caspase cleavage contribute to NMDA-induced neuronal apoptosis. *Proceedings of the National Academy of Sciences* **99**: 3974-3979

Otera H, Wang C, Cleland MM, Setoguchi K, Yokota S, Youle RJ, Mihara K (2010) Mff is an essential factor for mitochondrial recruitment of Drp1 during mitochondrial fission in mammalian cells. *The Journal of Cell Biology* **191**: 1141-1158

Papadia S, Soriano FX, Leveille F, Martel MA, Dakin KA, Hansen HH, Kaindl A, Sifringer M, Fowler J, Stefovskaja V, McKenzie G, Craighero M, Corriveau R, Ghazal P, Horsburgh K, Yankner BA, Wyllie DJ, Ikonomidou C, Hardingham GE (2008) Synaptic NMDA receptor activity boosts intrinsic antioxidant defenses. *Nat Neurosci* **11**: 476-487

Pham AH, Meng S, Chu QN, Chan DC (2012) Loss of Mfn2 results in progressive, retrograde degeneration of dopaminergic neurons in the nigrostriatal circuit. *Human Molecular Genetics* **21**: 4817-4826

Pich S, Bach D, Briones P, Liesa M, Camps M, Testar X, Palacín M, Zorzano A (2005) The Charcot-Marie-Tooth type 2A gene product, Mfn2, up-regulates fuel oxidation through expression of OXPHOS system. *Human Molecular Genetics* **14**: 1405-1415

Reynolds I, Hastings T (1995) Glutamate induces the production of reactive oxygen species in cultured forebrain neurons following NMDA receptor activation. *The Journal of Neuroscience* **15**: 3318-3327

Rintoul GL, Filiano AJ, Brocard JB, Kress GJ, Reynolds IJ (2003) Glutamate Decreases Mitochondrial Size and Movement in Primary Forebrain Neurons. *The Journal of Neuroscience* **23**: 7881-7888

Santalucia T, Moreno H, Palacin M, Yacoub MH, Brand NJ, Zorzano A (2001) A novel functional co-operation between MyoD, MEF2 and TRalpha1 is sufficient for the induction of GLUT4 gene transcription. *Journal of molecular biology* **314**: 195-204

Sattler R, Xiong Z, Lu W-Y, Hafner M, MacDonald JF, Tymianski M (1999) Specific Coupling of NMDA Receptor Activation to Nitric Oxide Neurotoxicity by PSD-95 Protein. *Science* **284**: 1845-1848

Sebastián D, Hernández-Alvarez MI, Segalés J, Sorianello E, Muñoz JP, Sala D, Waget A, Liesa M, Paz JC, Gopalacharyulu P, Orešič M, Pich S, Burcelin R, Palacín M, Zorzano A (2012) Mitofusin 2 (Mfn2) links mitochondrial and endoplasmic reticulum function with insulin signaling and is essential for normal glucose homeostasis. *Proceedings of the National Academy of Sciences* **109**: 5523-5528

Segales J, Paz JC, Hernandez-Alvarez MI, Sala D, Munoz JP, Noguera E, Pich S, Palacin M, Enriquez JA, Zorzano A (2013) A form of Mitofusin 2 (Mfn2) lacking the transmembrane domains and the C-terminal end stimulates metabolism in muscle and liver cells. *American journal of physiology Endocrinology and metabolism*

Smirnova E, Shurland D-L, Ryazantsev SN, van der Blik AM (1998) A Human Dynamin-related Protein Controls the Distribution of Mitochondria. *The Journal of Cell Biology* **143**: 351-358

Song Z, Chen H, Fiket M, Alexander C, Chan DC (2007) OPA1 processing controls mitochondrial fusion and is regulated by mRNA splicing, membrane potential, and Yme1L. *The Journal of Cell Biology* **178**: 749-755

Sorianello E, Soriano FX, Fernández-Pascual S, Sancho A, Naon D, Vila-Caballer M, González-Navarro H, Portugal J, Andrés V, Palacín M, Zorzano A (2012) The promoter activity of human Mfn2 depends on Sp1 in vascular smooth muscle cells. *Cardiovascular Research* **94**: 38-47

Soriano FX, Liesa M, Bach D, Chan DC, Palacín M, Zorzano A (2006) Evidence for a Mitochondrial Regulatory Pathway Defined by Peroxisome Proliferator-Activated Receptor-γ Coactivator-1α, Estrogen-Related Receptor-α, and Mitofusin 2. *Diabetes* **55**: 1783-1791

Soriano FX, Martel M-A, Papadia S, Vaslin A, Baxter P, Rickman C, Forder J, Tymianski M, Duncan R, Aarts M, Clarke PGH, Wyllie DJA, Hardingham GE (2008) Specific Targeting of Pro-Death NMDA Receptor Signals with Differing Reliance on the NR2B PDZ Ligand. *The Journal of Neuroscience* **28**: 10696-10710

Stout AK, Raphael HM, Kanterewicz BI, Klann E, Reynolds IJ (1998) Glutamate-induced neuron death requires mitochondrial calcium uptake. *Nat Neurosci* **1**: 366-373

Tanaka A, Cleland MM, Xu S, Narendra DP, Suen D-F, Karbowski M, Youle RJ (2010) Proteasome and p97 mediate mitophagy and degradation of mitofusins induced by Parkin. *The Journal of Cell Biology* **191**: 1367-1380

Vaslin A, Puyal J, Clarke PGH (2009) Excitotoxicity-induced endocytosis confers drug targeting in cerebral ischemia. *Annals of Neurology* **65**: 337-347

Wang Z, Jiang H, Chen S, Du F, Wang X (2012) The mitochondrial phosphatase PGAM5 functions at the convergence point of multiple necrotic death pathways. *Cell* **148**: 228-243

Wappler EA, Institoris A, Dutta S, Katakam PV, Busija DW (2013) Mitochondrial dynamics associated with oxygen-glucose deprivation in rat primary neuronal cultures. *PLoS one* **8**: e63206

Westermann B (2010) Mitochondrial fusion and fission in cell life and death. *Nature reviews Molecular cell biology* **11**: 872-884

Yoon Y, Krueger EW, Oswald BJ, McNiven MA (2003) The Mitochondrial Protein hFis1 Regulates Mitochondrial Fission in Mammalian Cells through an Interaction with the Dynamin-Like Protein DLP1. *Molecular and Cellular Biology* **23**: 5409-5420

Young KW, Piñon LGP, Bampton ETW, Nicotera P (2010) Different pathways lead to mitochondrial fragmentation during apoptotic and excitotoxic cell death in primary neurons. *Journal of Biochemical and Molecular Toxicology* **24**: 335-341

Yu S-W, Wang H, Poitras MF, Coombs C, Bowers WJ, Federoff HJ, Poirier GG, Dawson TM, Dawson VL (2002) Mediation of Poly(ADP-Ribose) Polymerase-1-Dependent Cell Death by Apoptosis-Inducing Factor. *Science* **297**: 259-263

Zhang L, Zhang ZG, Chopp M (2012) The neurovascular unit and combination treatment strategies for stroke. *Trends in pharmacological sciences* **33**: 415-422

Zhang SJ, Steijaert MN, Lau D, Schutz G, Delucinge-Vivier C, Descombes P, Bading H (2007) Decoding NMDA receptor signaling: identification of genomic programs specifying neuronal survival and death. *Neuron* **53**: 549-562

Zuchner S, Mersiyanova IV, Muglia M, Bissar-Tadmouri N, Rochelle J, Dadali EL, Zappia M, Nelis E, Patitucci A, Senderek J, Parman Y, Evgrafov O, Jonghe PD, Takahashi Y, Tsuji S, Pericak-Vance MA, Quattrone A, Battologlu E, Polyakov AV, Timmerman V, Schroder JM, Vance JM (2004) Mutations in the mitochondrial GTPase mitofusin 2 cause Charcot-Marie-Tooth neuropathy type 2A. *Nat Genet* **36**: 449-451

Figure legends

Figure 1. Mfn2 expression is reduced in excitotoxicity *in vitro* and *in vivo*. Western analysis of mitochondrial fusion/fission proteins. A) *In vitro* primary cortical neurons exposed to NMDA (30 μ M) for the indicated times and (B) densitometric analysis normalized to actin (n=3–6). C) *In vivo* brain extracts of rats subjected to MCAO plus 90 minutes of ipsilateral carotid clamp followed by clamp release for the indicated times and (D) densitometric analysis normalized to actin (n=3–7). Mean \pm s.e.m. in this and subsequent cases. *p<0.05 compared to control, two-tailed T-test.

Figure 2. Activation of Drp1 induces mitochondrial fragmentation. A) Representative images of neurons transfected with plasmid encoding mitochondriatargeted RFP (mtRFP) showing tubular or fragmented mitochondria. The white box indicates the high magnification area. Arrowhead points to the transfected neuron. Scale bar = 20 μ m. B) Time-course of NMDA-induced mitochondrial fragmentation. Neurons transfected with mtRFP were treated with NMDA (30 μ M) for the indicated times and mitochondrial morphology was analyzed (n=3-8). *p<0.05 compared to control, one-way ANOVA followed by Bonferroni post hoc test. C) NMDA induces increased Drp1 translocation to mitochondria. Neurons were transfected with plasmids encoding GFP-Drp1 and mtRFP. After 48 h neurons were stimulated with NMDA (30 μ M) for 1 hour or left unstimulated, fixed and visualized under a confocal microscope. Brightness and contrast has been adjusted in the merged image to visualize GFP signal in the control condition. Scale bar yellow = 20 μ m, white = 4 μ m. D) Genetic and pharmacological inhibitors of Drp1 block mitochondrial fragmentation.

Neurons were transfected with plasmids encoding mtRFP and Drp1-K38A or control (globin). After 48 hours neurons were stimulated with NMDA (30 μ M) for 1 hour and mitochondrial morphology was analyzed (n=3) or they were pre-treated for 1 hour before NMDA stimulation with mdiv-1 (25 μ M) or 7-Nitroindazole ((7-Ni) at 5 μ M in Arg free medium). *p<0.05, one-way ANOVA followed by Bonferroni post hoc test.

Figure 3. Mfn2 intervenes in an irreversible delayed phase of mitochondrial fragmentation. A) Secondary mitochondrial fragmentation after NMDA wash-out. Neurons were transfected with mtRFP. After 48 h neurons were stimulated with NMDA (30 μ M) for 1 hour and washed out for the indicated times and mitochondrial morphology was analyzed (n=4–5). *p<0.05, one-way ANOVA followed by Bonferroni post hoc test. B) Mfn2 is reduced after NMDA wash-out. Western and densitometric analysis of neurons treated with NMDA (30 μ M) for 1 hour and washed out for 3 additional hours (n=4). *p<0.05, two-tailed T-test. C) Representative western blot and densitometric analysis of neurons transduced with AAV producing shRNA against Mfn2 or scrambled (n=4). *p<0.05, one-way ANOVA followed by Bonferroni post hoc test. D) Mfn2 knockdown causes mitochondrial fragmentation. Analysis of mitochondrial morphology of neurons transfected with plasmids shMfn2 or sh-sc and mtRFP (n=4). *p<0.05, two-tailed T-test. E) Mfn2 blocks the delayed phase of NMDA-induced mitochondrial fragmentation. Neurons transfected with plasmids encoding mtRFP and Mfn2 or globin (CT) were treated with NMDA (30 μ M) for 1 hour and washed out for 3 additional hours and mitochondrial morphology was analyzed (n=3). *p<0.05, one-way ANOVA followed by Bonferroni post hoc test.

Figure 4 Mfn2 downregulation causes mitochondrial dysfunction and altered Ca²⁺ homeostasis and sensitizes neurons to excitotoxic damage. A) Loss of mitochondrial membrane potential in neurons transfected with sh-Mfn2 or sh-sc and treated with NMDA (15 μ M; arrow) was determined by measuring TMRM fluorescence. The values were normalized to surrounding untransfected neurons (n=19–21 neurons analyzed in five independent experiments). *p<0.05, two-tailed T-test. B) Determination of intracellular Ca²⁺ in cortical neurons transduced with AAV producing sh-Mfn2 or sh-sc and treated with NMDA (15 μ M) (n=3). C) Histograms show the average intracellular Ca²⁺ levels 20 minutes before and after NMDA application (15 μ M) (n=3). *p<0.05, one-way ANOVA followed by Bonferroni post hoc test. D) Neurons transfected with plasmids expressing sh-Mfn2 or sh-sc were treated with subtoxic doses of NMDA (15 μ M) for 6 hours. Death was analyzed by fixing cells, DAPI-staining and counting pyknotic nuclei of the transfected neurons (n=5). *p<0.05, two-tailed T-test.

Figure 5. Mfn2 is regulated at transcriptional level in excitotoxicity. Cortical neurons with or without pre-incubation with proteasome inhibitor MG-132 (10 μ M) were treated for 4 hours with NMDA (30 μ M) and Mfn2 levels were analyzed by western blot. A) Representative western and B) densitometric analysis (n=7). *p<0.05, one-way ANOVA followed by Bonferroni post hoc test. C) Cortical neurons were treated with NMDA (30 μ M) for the indicated times and mRNA expression was determined by real time qPCR. (n=4). *p<0.05, two-tailed T-test. Cortical neurons were treated with transcriptional inhibitor actinomycin D, translational inhibitor cycloheximide and NMDA (30 μ M) for 4 hours as indicated and Mfn2 protein

expression was analyzed by western blot. D) Representative western and E) densitometric analysis (n=4). *p<0.05, two-tailed T-test.

Figure 6. Excitotoxicity-mediated Mfn2 downregulation depends on MEF2. Time course of excitotoxicity dependent MEF degradation (A) in cortical neurons *in vitro* treated with NMDA (30 μ M) for 4 hours and (B) brain extracts of rats subjected to MCAO plus 90 minutes of ipsilateral carotid clamp followed by clamp release for the indicated times. C) Cortical neurons transduced with AAV expressing MEF2-DN have lower Mfn2 levels than AAV-GFP or non transduced neurons. D) Mitochondrial morphology in cortical neurons transfected with the indicated expression vectors (n=4–5). *p<0.05, one-way ANOVA followed by Bonferroni post hoc test. E) Mitochondrial membrane potential of neurons expressing the indicated vectors (n=9 cells from three independent experiments). F) Cortical neurons transduced with AAV expressing MEF2-DN or GFP (control) were treated with NMDA (30 μ M) for 4 hours and Mfn2 mRNA expression was determined by qRT-PCR (n=5). *p<0.05, one-way ANOVA followed by Bonferroni post hoc test.

Figure 7. MEF2 directly regulates basal Mfn2 expression in neurons. A) Luciferase-based reporter of *Mfn2* promoter in cortical neurons (left) or 10T1/2 cell line (right) and SESN2 promoter in cortical neurons (center) in control or over-expressing MEF2-DN (n=3-9). *p<0.05 compared to control, two-tailed T-test. B) Deletion analysis of a luciferase-based reporter of the *Mfn2* promoter in 10T1/2 cells co-expressed with control or MEF2 plasmids (n=3). *p<0.05, two-tailed T-test. C) Effect of putative MEF2 binding site mutations on MEF2-dependent induction of the *Mfn2* promoter in 10T1/2 cells (n=3). *p<0.05 compared to control, two-tailed T-test. D) EMSA

performed with nuclear extracts of HeLa cells overexpressing MEF2 and radiolabeled probe encoding BOX 2 from Mfn2 promoter. Retardation complexes are indicated with arrows. Excess of cold oligonucleotide, mutated oligonucleotide or oligonucleotide of the Glut4 gene that contains a MEF2 binding site was used to compete. Radiolabeled probe containing mutated BOX 2 did not produce retardation complexes. E) Supershift was performed using MEF2 polyclonal antibody. Pre-immune serum was used as a negative control.* indicates nonspecific binding of the probe to MEF2 antibody. F) HeLa cells were transfected with a MEF2A expression vector or an irrelevant expression vector (CT). ChIP carried out using MEF2A polyclonal antibody. Pre-immune serum was used as a negative control. The input and immunoprecipitated DNA was used as a template for PCR with primers flanking the BOX 2 site on the Mfn2 gene. Primers amplifying a region of cyclophilin gene were used as the negative control. G) ChIP in cortical neurons untreated or treated with NMDA (30 μ M) for 4 hours using the indicated antibodies (n=4). *p<0.05, one-way ANOVA followed by Bonferroni post hoc test.

Figure 8. Proposed model for the changes in mitochondrial morphology and vulnerability in excitotoxic conditions. Under basal conditions MEF2 binds Mfn2 promoter and regulates its gene expression resulting in mainly tubular mitochondria. In excitotoxic conditions Drp1 translocates to mitochondria and mediates rapid, reversible mitochondrial fission. An increase in cytosolic Ca^{2+} produces MEF2 degradation and Mfn2 gene expression is consequently downregulated, producing a delayed long term effect on mitochondrial morphology. Reduced expression of Mfn2 impairs mitochondrial function, which causes dysregulation of Ca^{2+} homeostasis and sensitizes neurons to subtoxic excitotoxic insults.

Figure 1

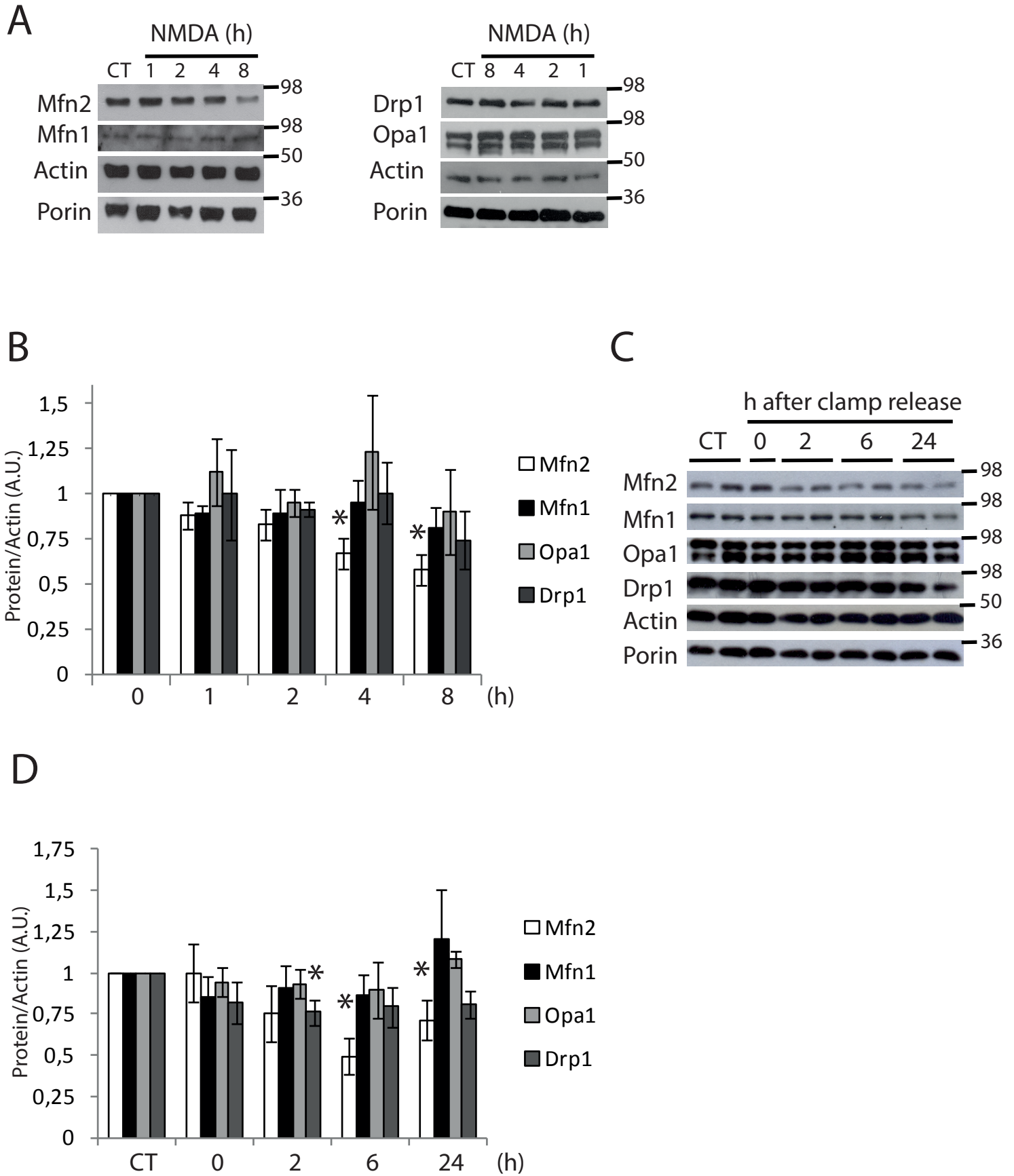


Figure 2

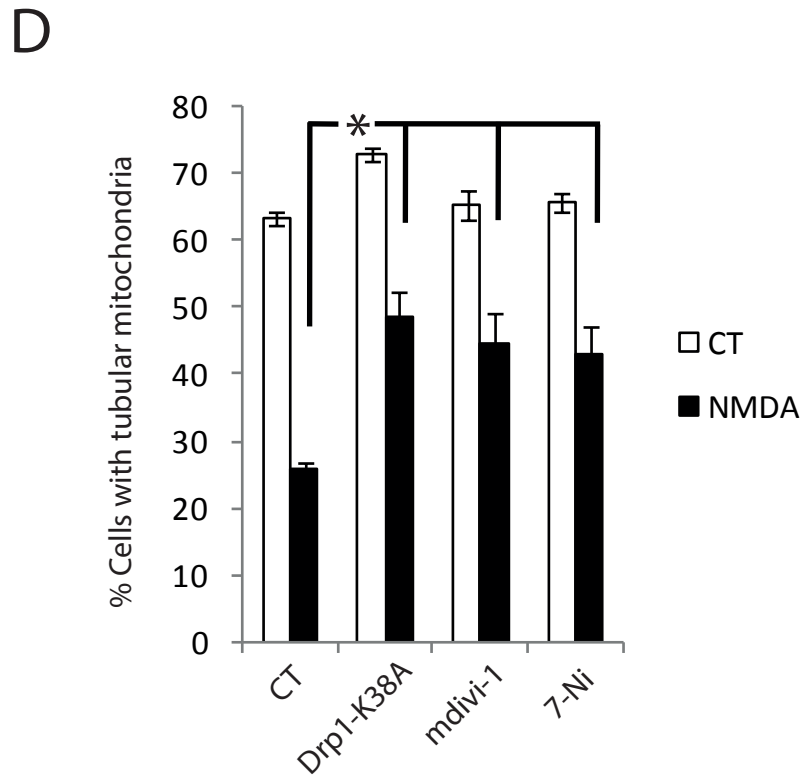
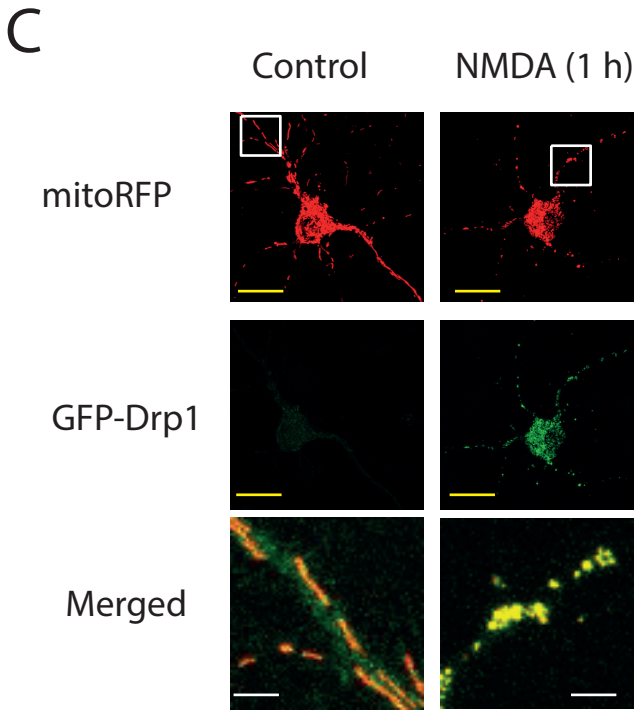
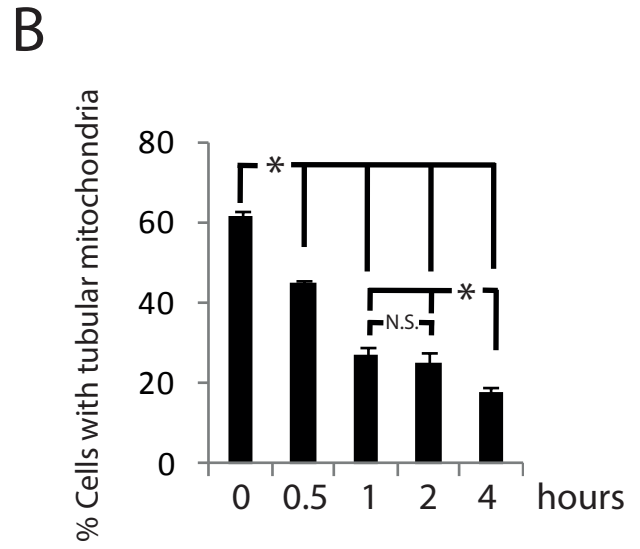
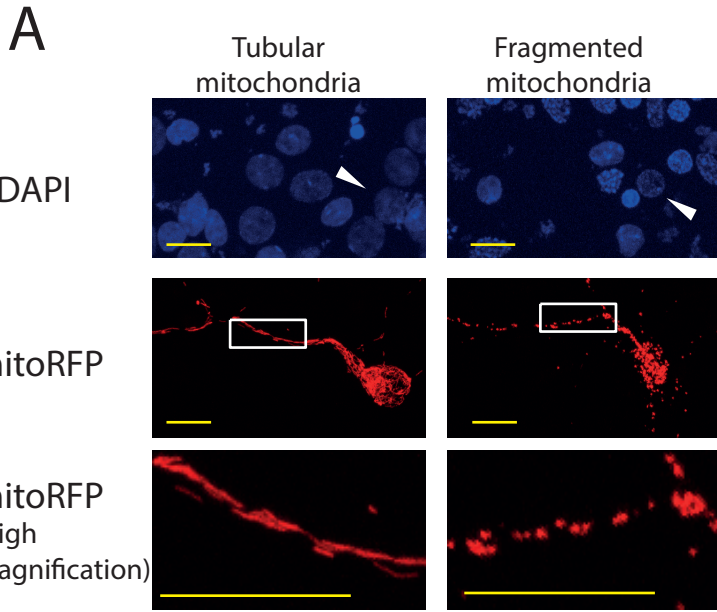


Figure 3

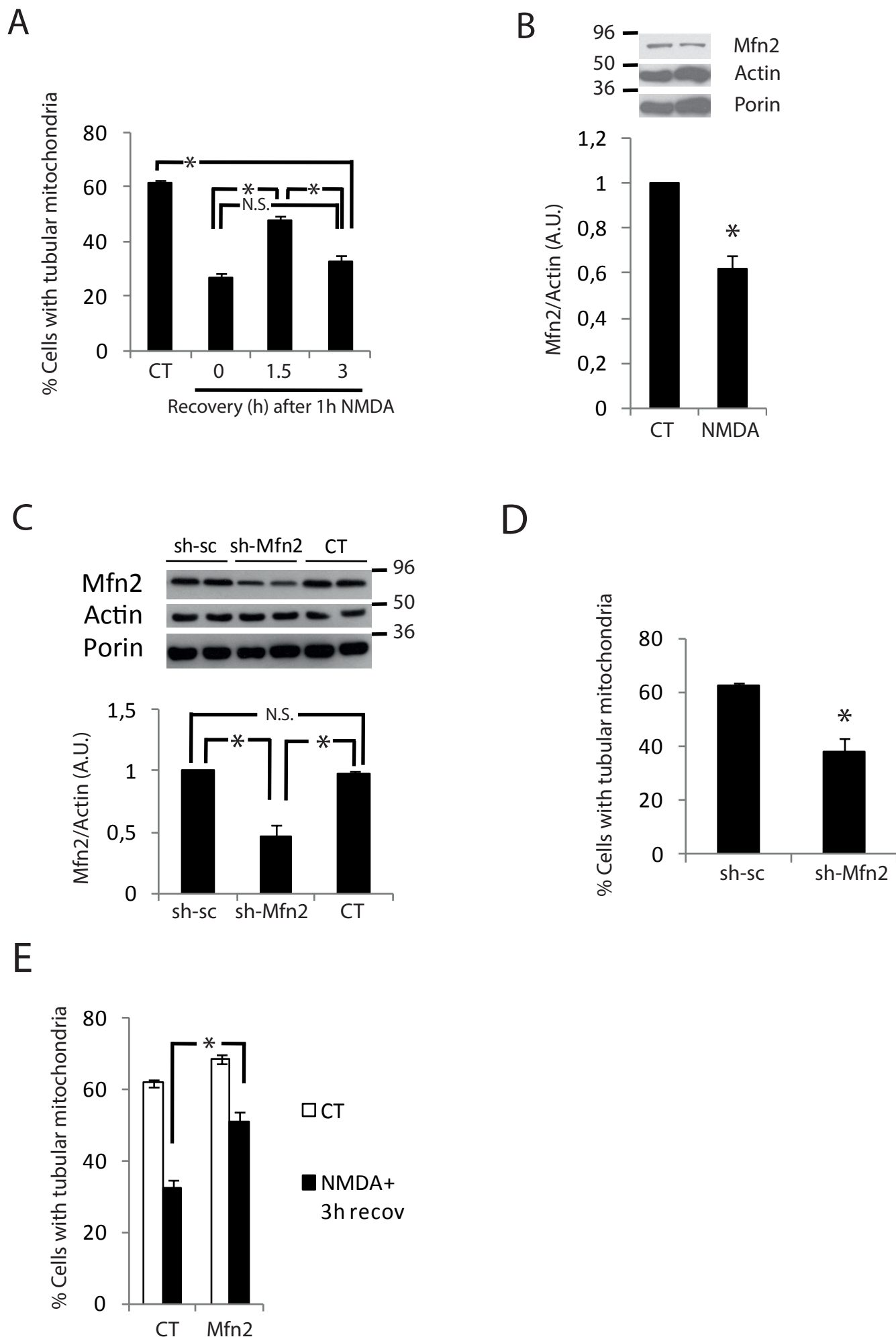
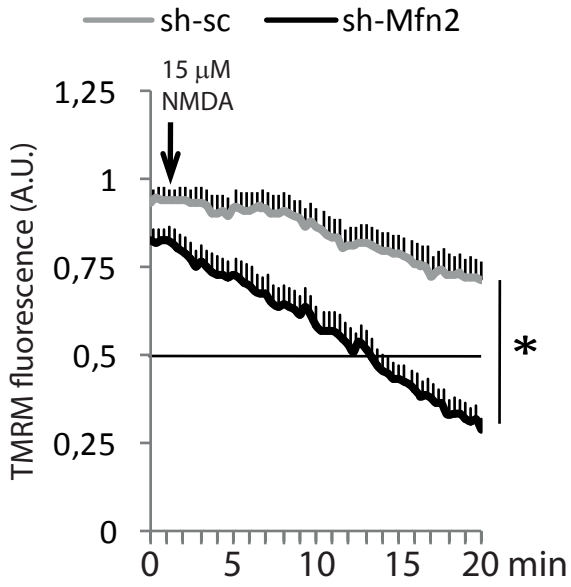
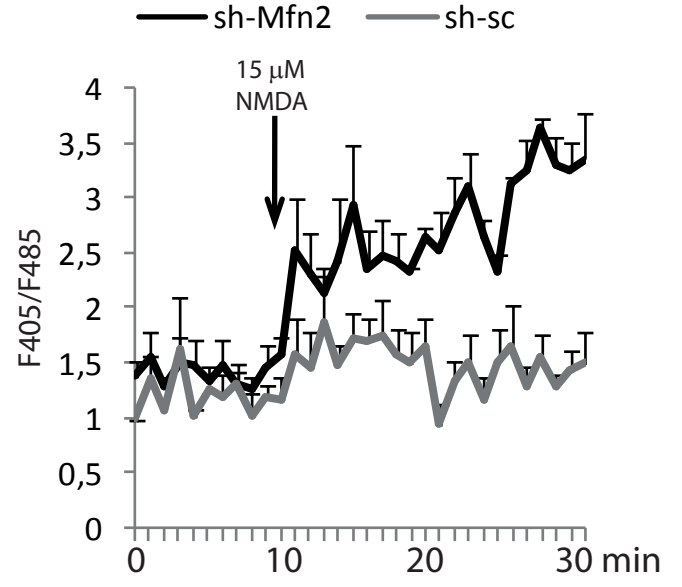


Figure 4

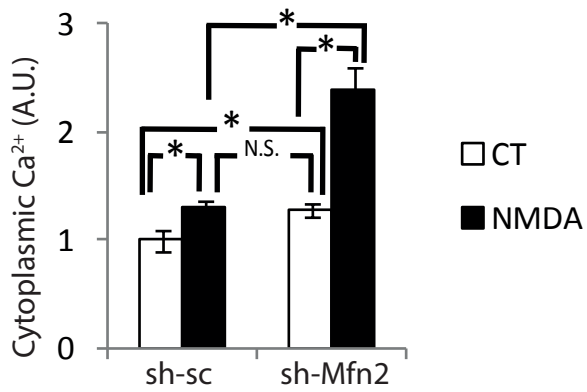
A



B



C



D

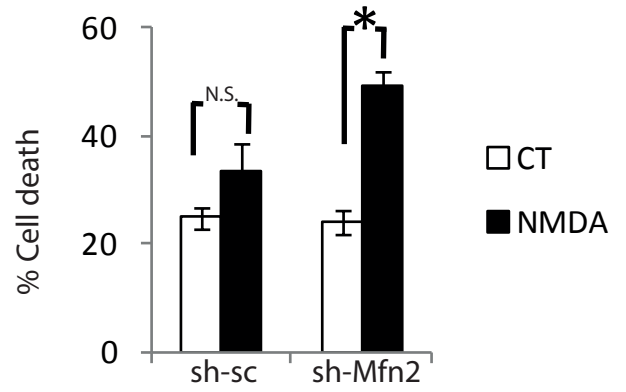
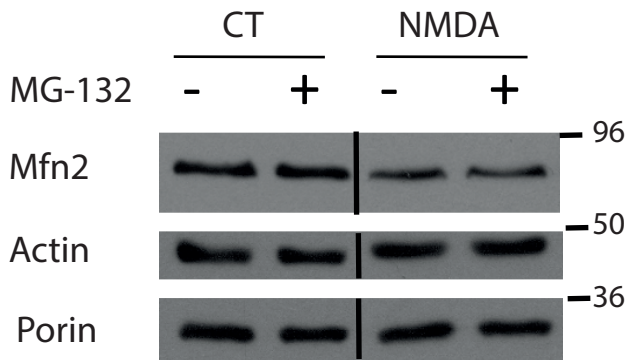
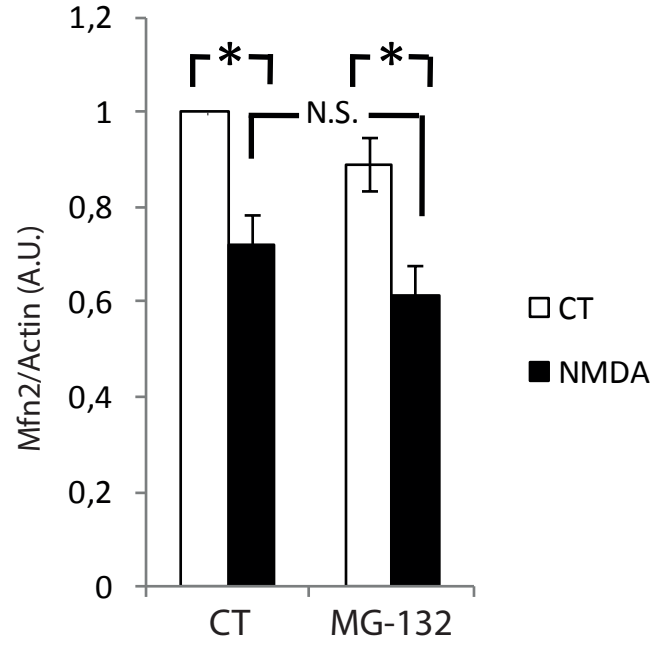


Figure 5

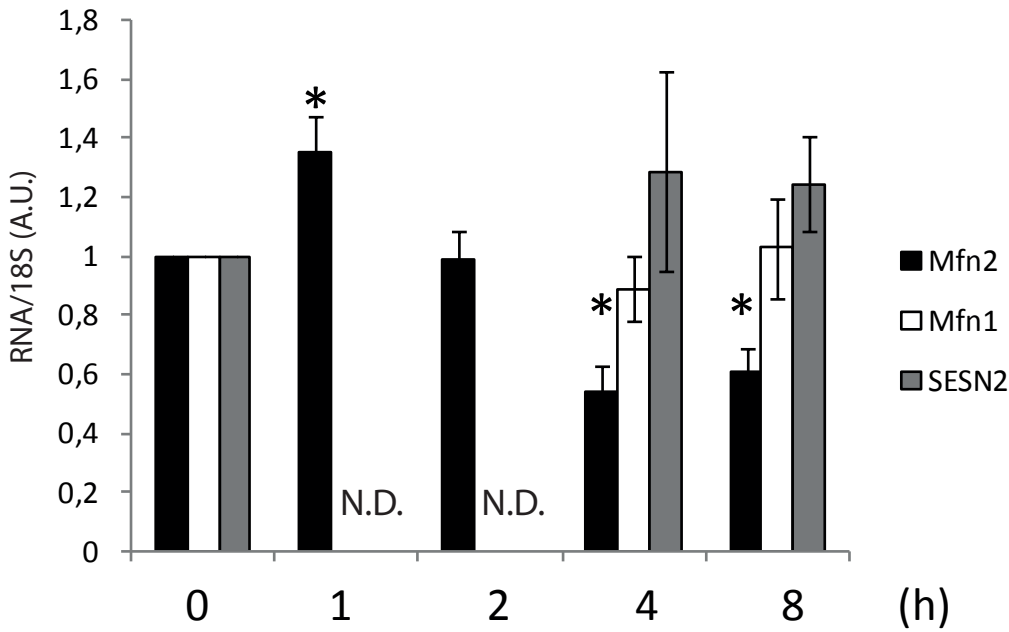
A



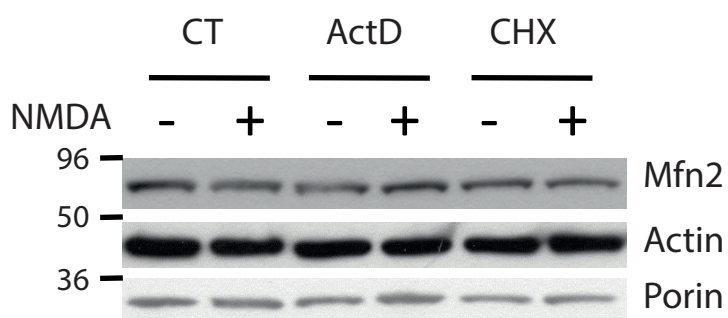
B



C



D



E

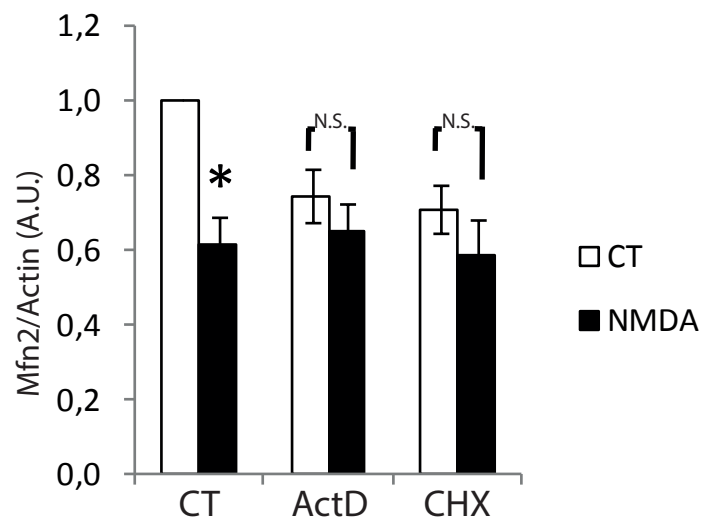


Figure 6

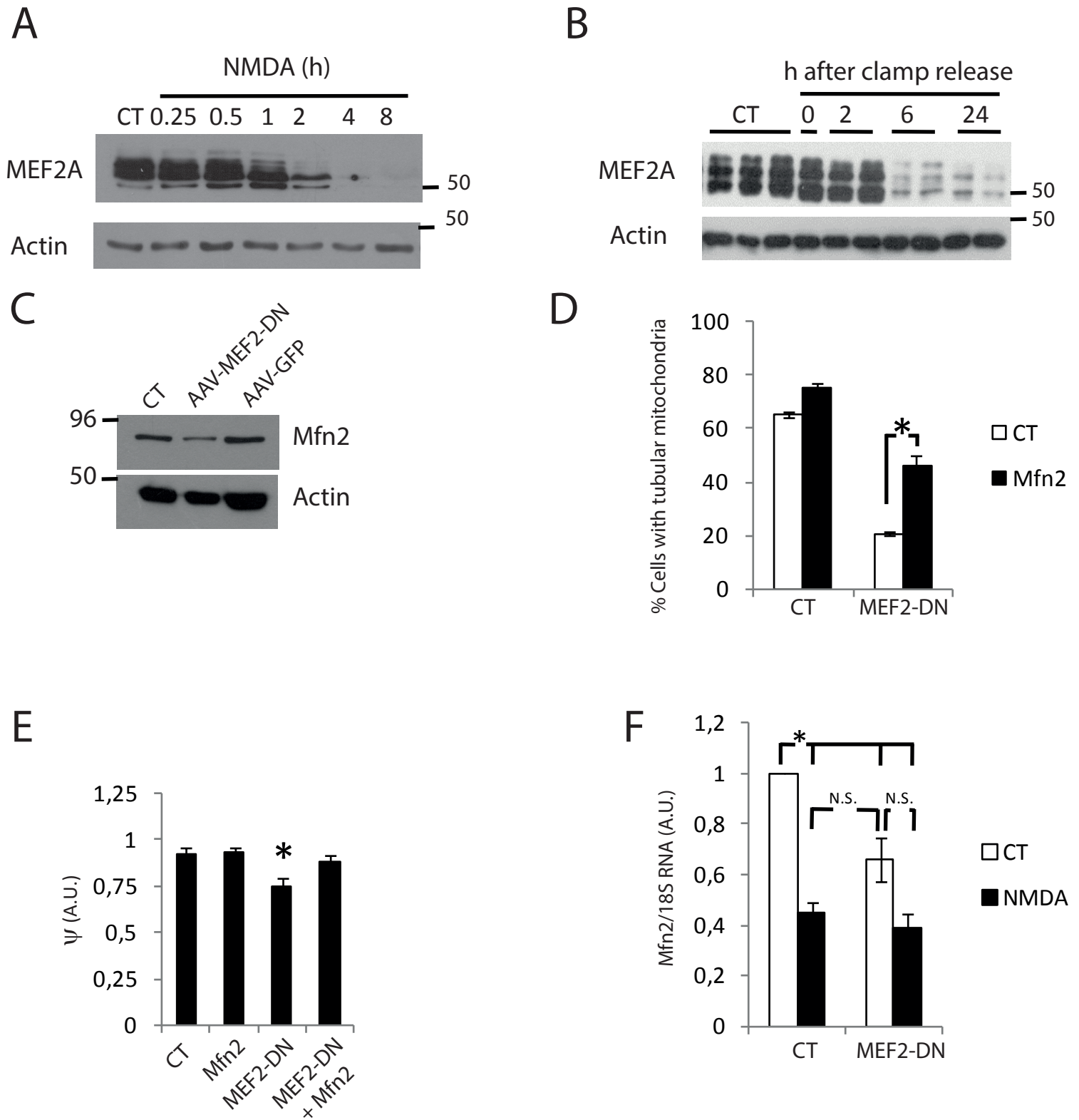
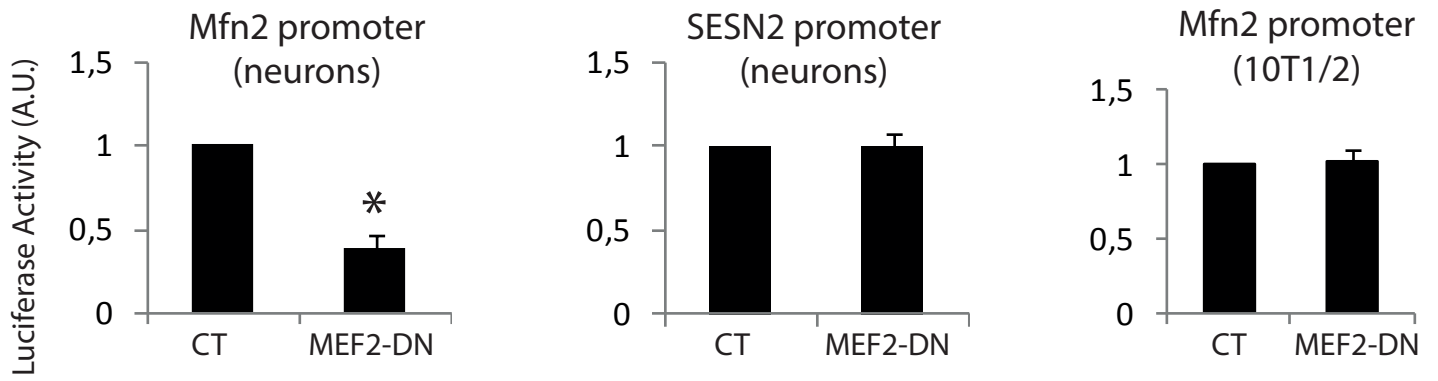
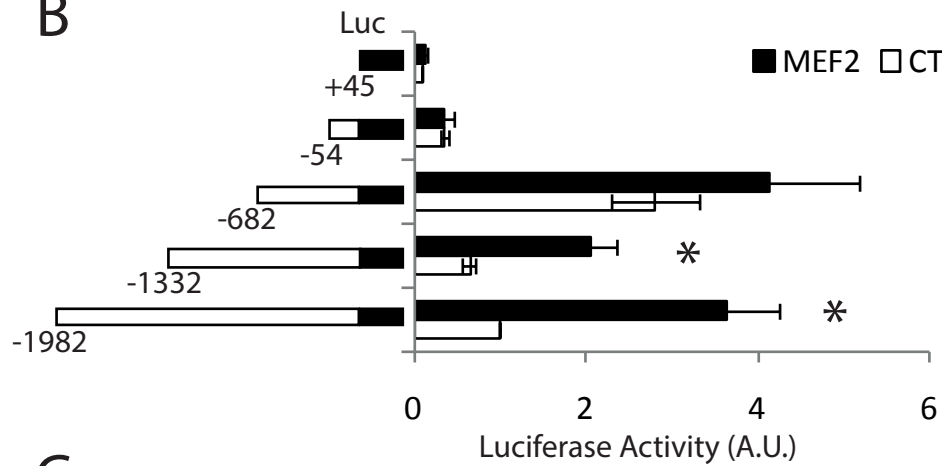


Figure 7

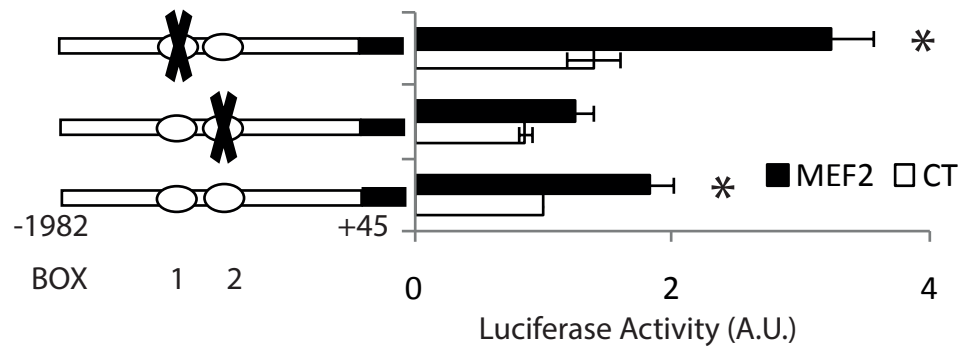
A



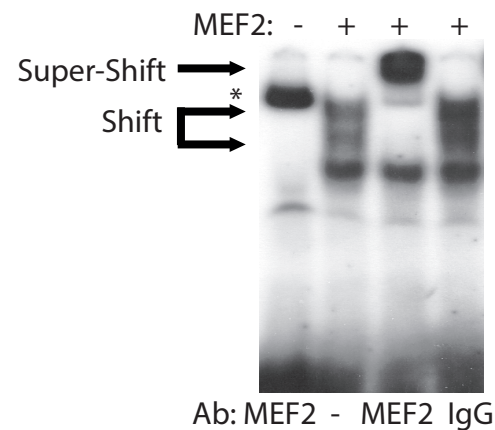
B



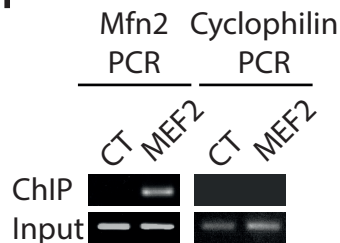
C



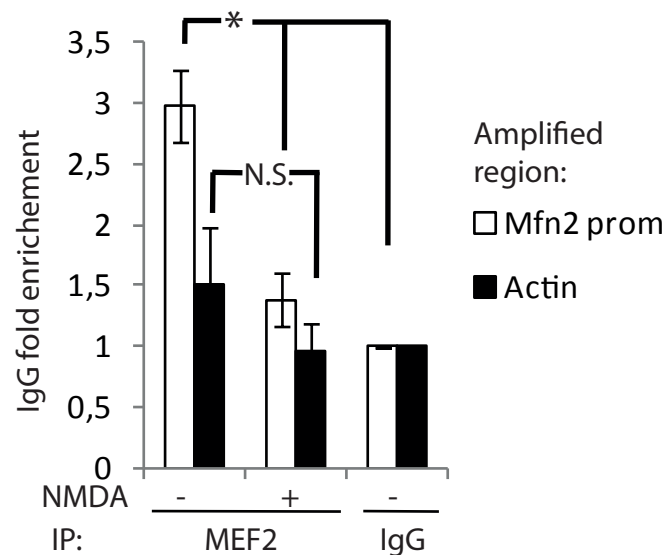
E



F



G



D

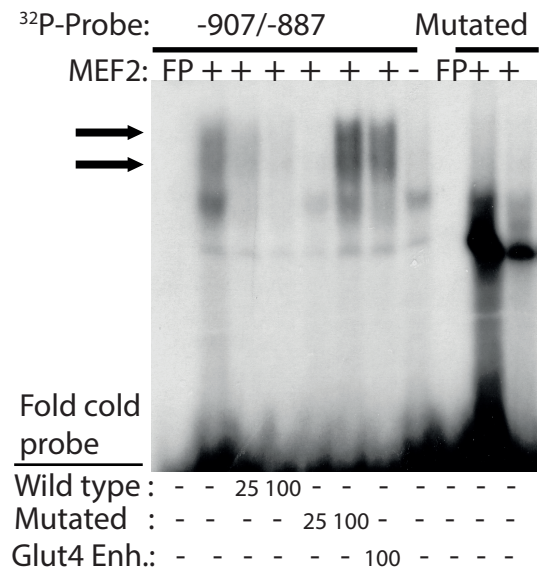


Figure 8.

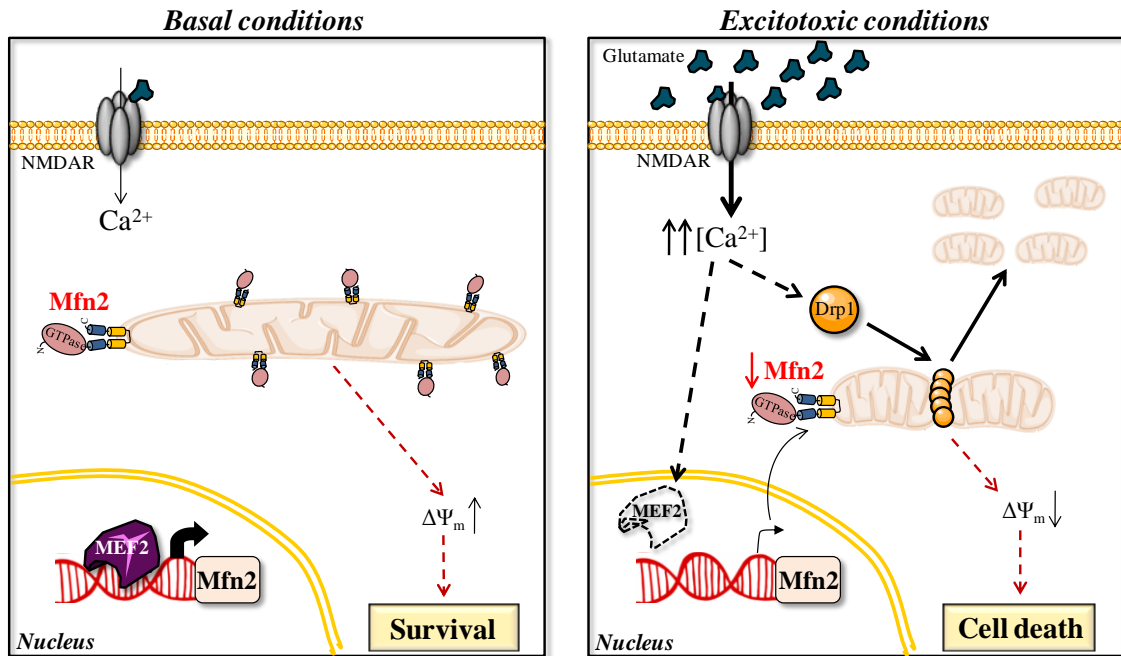
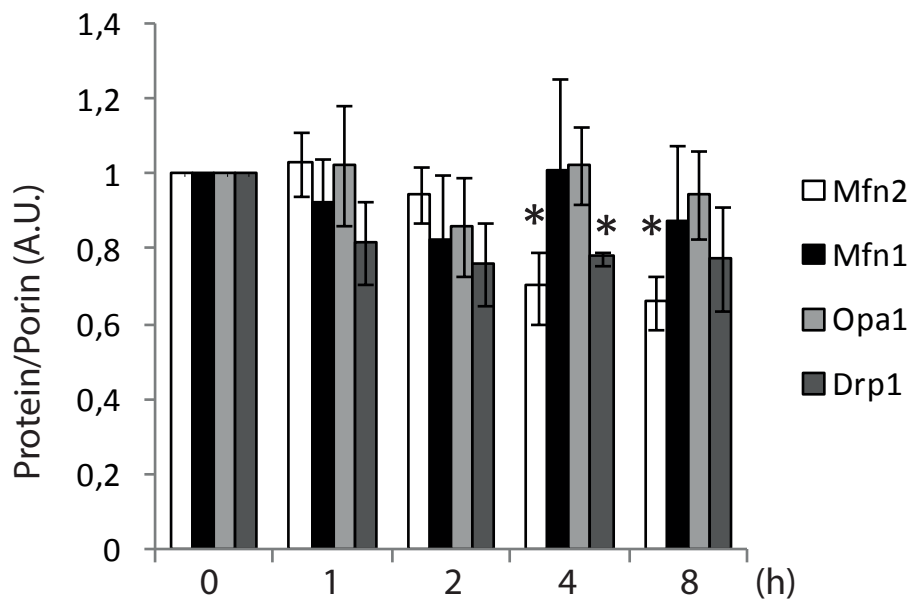
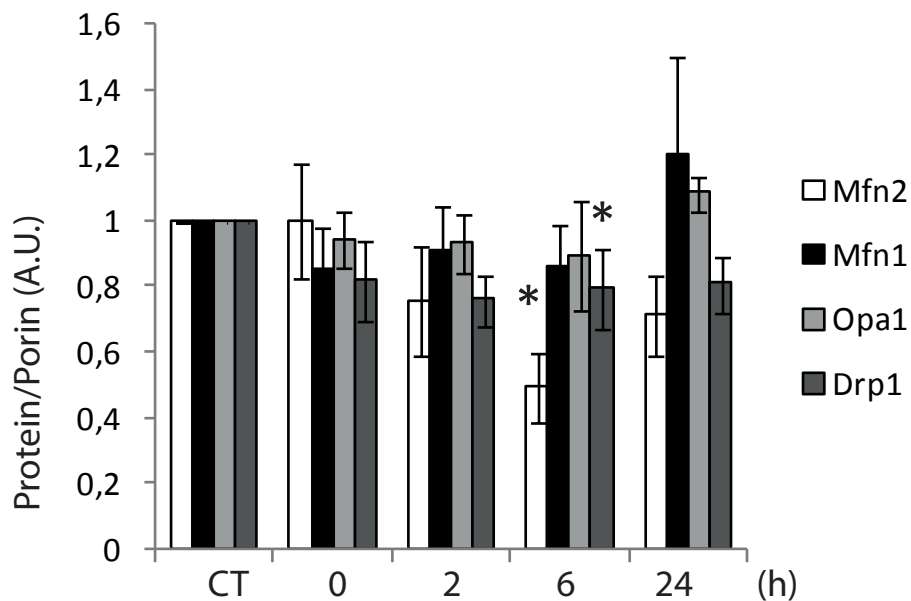


Figure S1 (related to Figure 1)

A

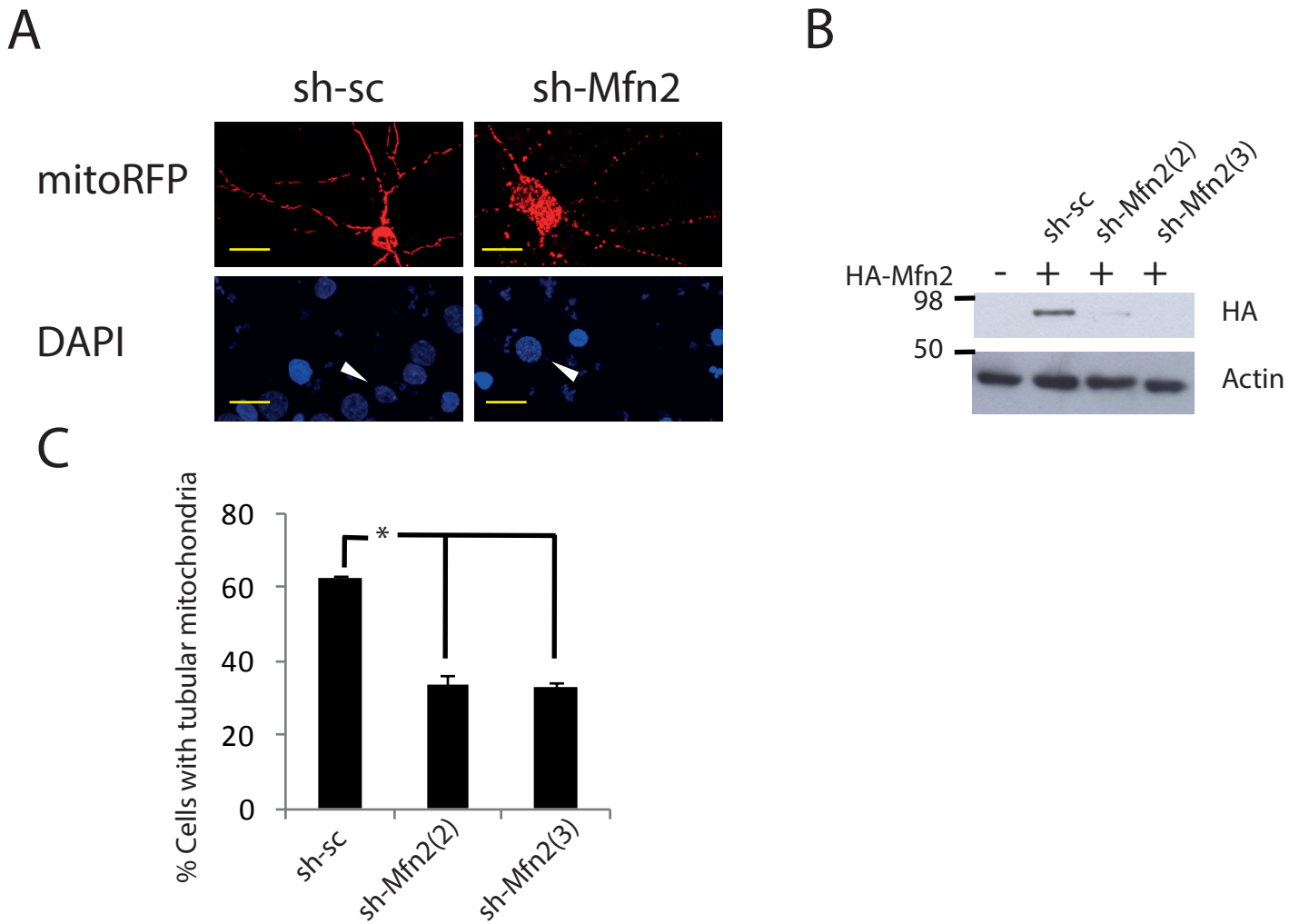


B



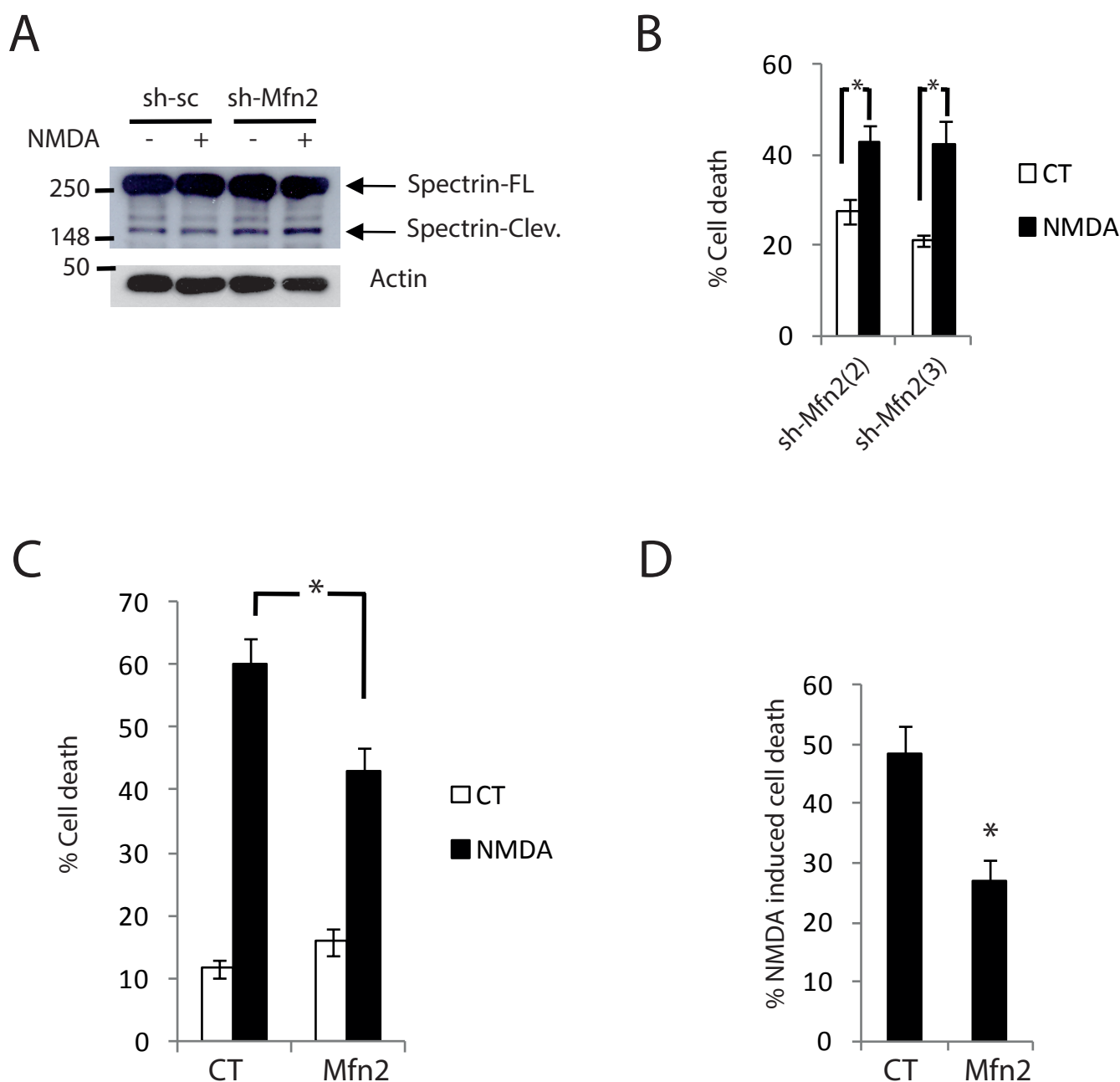
Supplementary Figure S1. Densitometric analysis normalized to porin of western blots of the indicated mitochondrial fusion/fission proteins: A) in vitro primary cortical neurons exposed to NMDA (30 μ M) for the indicated times (n=3–6). B) In vivo brain extracts of rats subjected to MCAO plus 90 minutes of ipsilateral carotid clamp followed by clamp release for the indicated times (n=3–7). *p<0.05 compared to control, two-tailed T-test.

Figure S2 (related to Figure 3)



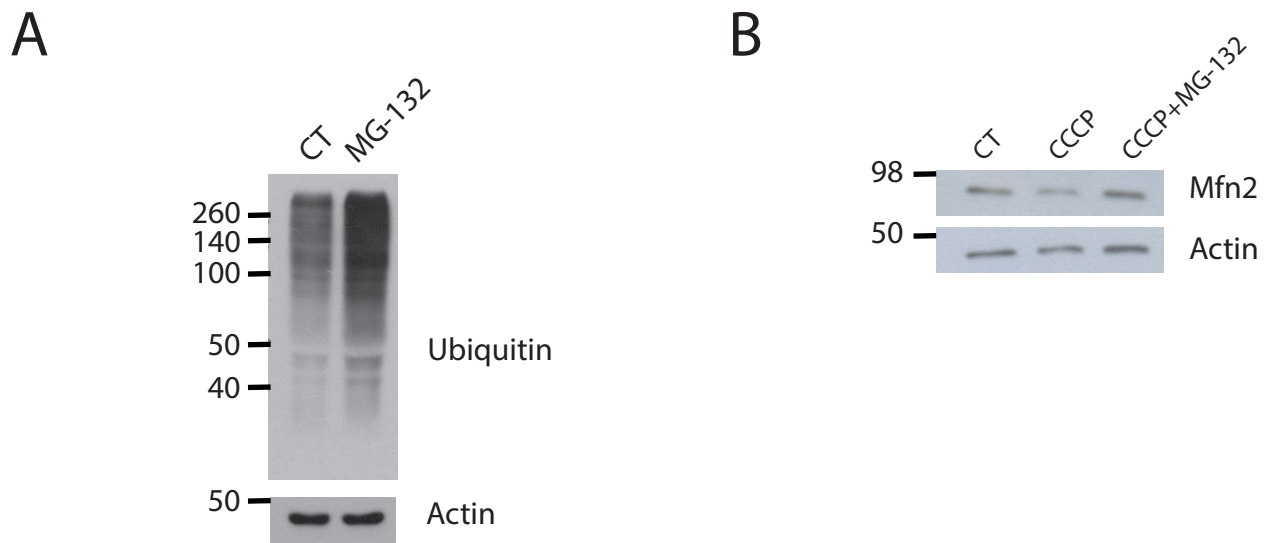
Supplementary Figure S2. A) Representative images of neurons transfected with mtRFP plus plasmids producing sh-sc or sh-Mfn2. White arrowheads indicate the transfected neurons. Scale bar=20 μ m. B) HEK293 cells were transfected with plasmids encoding HA-Mfn2 plus shRNA targeted against different sequences of Mfn2 (sh-Mfn2) or sh-sc. After 48 hours protein was harvested and subjected to western blot. C) Analysis of mitochondrial morphology in neurons expressing different sh-Mfn2 or sh-sc (n=3). *p<0.05, two-tailed T-test.

Figure S3 (related to Figure 4)



Supplementary Figure S3. A) Representative western blot showing spectrin full length (spectrin-FL) and spectrin cleaved (spectrin-clev.) in neurons expressing sh-sc or sh-Mfn2 after 30 minutes of treatment with subtoxic NMDA (15 μ M). B) Cortical neurons were transfected with plasmids expressing sh-Mfn2 or sh-sc. After 48 hours neurons were treated with NMDA (15 μ M) for 6 hours. Neuronal death was analyzed (n=6). * p <0.05, two-tailed T-test. C) Cortical neurons were transfected with plasmids expressing Mfn2 or control (globin). After 48 h neurons were exposed to NMDA (30 μ M) for 6 hours. Neuronal death was analyzed (n=6). * p <0.05, one-way ANOVA followed by Bonferroni post hoc test. D) NMDA-dependent cell death in neurons expressing control (globin) or Mfn2 plasmid. Calculated by subtracting the basal cell death from the total cell death in C. * p <0.05, two-tailed T-test.

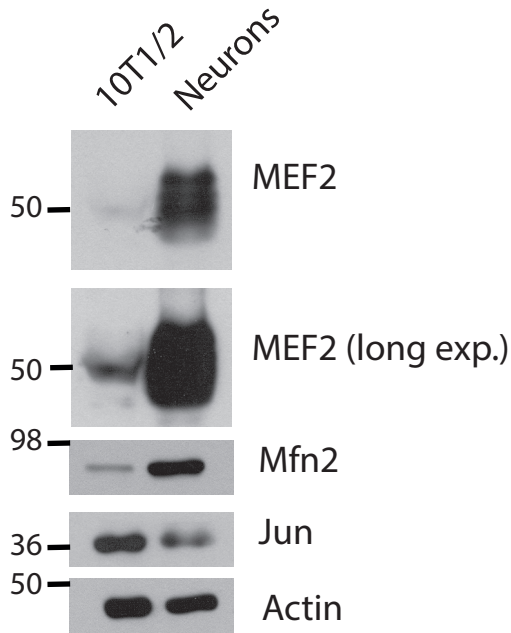
Figure S4 (related to Figure 5)



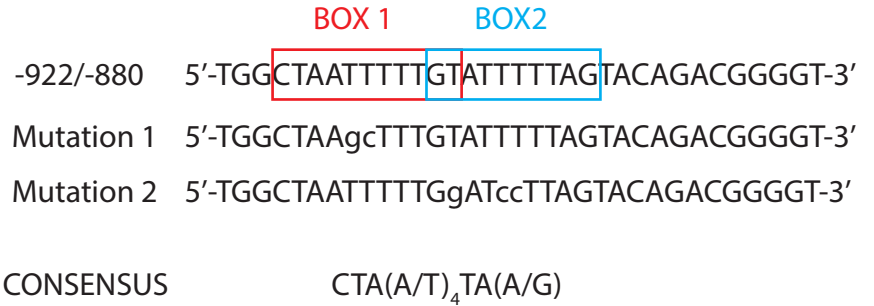
Supplementary Figure S4. A) MG-132 promotes accumulation of ubiquitinated proteins in neurons. Western blot showing ubiquitinated proteins in cortical neurons after 4 hours of treatment with 10 μ M MG-132. Actin was used as a loading control. B) CCCP dependent degradation of Mfn2 is blocked by the proteasome inhibitor MG-132. Cortical neurons were treated with CCCP (10 μ M) for 1 h in the absence or presence of MG-132 (10 μ M).

Figure S5 (related to figure 7)

A



B



C

-2352 TGTGGTTCCTCTGTAAAAGCCATCTCTCTTGGCCCCAGCCATATTTATTTATGGCGTGT

-2292 GGTTGATGCACACATGTCATGGCTCTCGTATGGAGGTTTAGGGGACAACCTTTTTACGAGT

-2232 AGGTTCTTTCCTTCCATCATGTGGGTTCCTGGAGATGGAATTCAAGTTGGCAGGCTTGGT

-2172 AGCAGCCATCTGTACCTACTGAGCCATTTTGTGACCAACCACTATTAGCTGTAGTTTTAGA

-2112 AGTAAAAAGAAATGGGAGTTTAATTAAGATAATGTATTTTATTAGTCGAGCGAATCCAA

-2052 AGTTATAGCAACATATCAATATGAAAACATTAGTAAGGTAGTTTGCATTTCTTTTAATA

-1992 ATAAATATTGGGGCATCTCTCTACAGCAACTACATTTTCAGGTCCTCAGTAGCTACAGGTG

Supplementary Figure S5. A) Western blot analysis to compare the expression of the indicated proteins in primary cortical neurons and 10T1/2 cells. B) Sequence of the two putative MEF2 binding sites found in the Mfn2 human promoter. The mutations of these sequences are in lower case. C) Sequence of the region between -2352/-1392 with respect to the transcription start site of the Mfn2 rat promoter. Shown in red are the putative MEF2 binding sites found using the PROMO and Patch public 1.0 programs. The region amplified in the ChIP experiments is shaded.